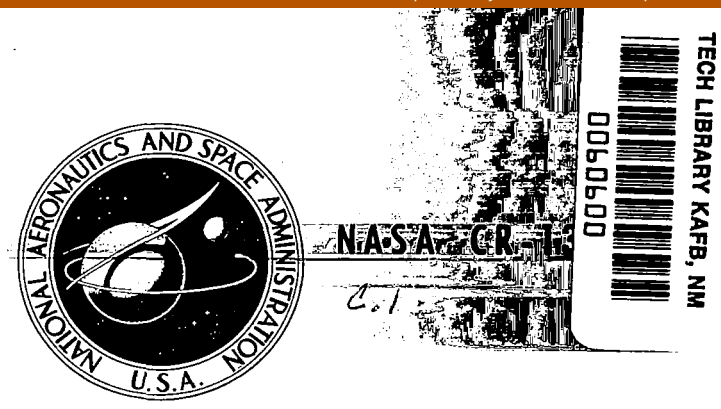

NASA CONTRACTOR REPORT

NASA CR-1326

SLOPE DIFFRACTION ANALYSIS OF TEM PARALLEL-PLATE GUIDE PATTERNS

by D. C. F. Wu and R. C. Rudduck

Prepared by
OHIO STATE UNIVERSITY
Columbus, Ohio
for Langley Research Center

NATIONAL AERONAUTICS AND SPACE ADMINISTRATION • WASHINGTON, D. C. • MAY 1969

NASA CR-1326

SLOPE DIFFRACTION ANALYSIS OF TEM PARALLEL-PLATE GUIDE PATTERNS

By D. C. F. Wu and R. C. Rudduck

Issued by Originator as Technical Report No. 1691-29

Prepared under Grant No. NGR 36-008-005 by
OHIO STATE UNIVERSITY
Columbus, Ohio

for Langley Research Center

NATIONAL AERONAUTICS AND SPACE ADMINISTRATION

For sale by the Clearinghouse for Federal Scientific and Technical Information
Springfield, Virginia 22151 – CFSTI price $3.00

ABSTRACT

The radiation pattern of a TEM mode parallel-plate waveguide is analyzed by wedge diffraction theory in conjunction with a slope correction term. This slope correction term is the diffraction by a conducting wedge due to an incident wave with sinusoidal amplitude variation over the wave front. Such a wave is referred to as a slope wave. The slope diffraction takes into account the nonuniform wave in calculating second-order diffractions for the open-ended guide. The slope correction term provides an improvement in the accuracy of the pattern in the region near the plane of the aperture as compared to the previous wedge diffraction calculations.

TABLE OF CONTENTS

SLOPE DIFFRACTION ANALYSIS OF TEM PARALLEL-PLATE GUIDE PATTERNS

I. INTRODUCTION

Radiation pattern analysis is a primary tool in the design of antennas. Consequently, the development and improvement of methods of analysis are of particular interest to the antenna designer. Small aperture antennas such as open-ended waveguides and slot antennas are of particular interest in applications for missiles, space craft, and airborne and reentry vehicles. The idealized two dimensional parallel-plate waveguide which is treated below provides insight into the diffraction behavior of practical three-dimensional antennas. The research reported here introduces a slope correction term which provides an improvement in the accuracy of the parallel-plate guide pattern as compared to the previous wedge diffraction calculations.[1]

The radiation pattern of the parallel-plate waveguide shown in Fig. 1 is considered in this report. The wedge angles WA1 and WA2 may be adjusted for various mounting configurations, and the guide is truncated perpendicularly to the guide axis as shown in Fig. 1. Only the TEM waveguide mode is considered here; in this mode an incident plane wave propagates parallel to the axis of the guide with polarization perpendicular to the waveguide walls.

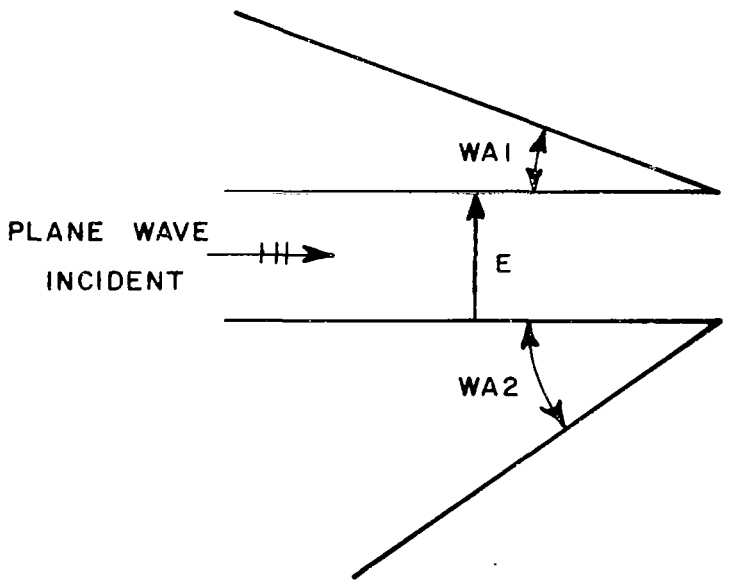

Fig. 1 - Geometry of a Parallel-Plate Guide

The TEM mode radiation pattern of a parallel-plate waveguide was analyzed previously by wedge diffraction theory.[1] In this method, the incident plane wave causes singly diffracted waves to emanate from each edge. Doubly diffracted waves are produced by the incidence of the singly diffracted waves on the opposite edges. Each doubly diffracted wave is approximated as the diffraction by an isotropic, cylindrical wave incident on the edge. This approximation of the nonisotropic, singly diffracted wave as an isotropic wave causes inaccuracy in the radiation pattern in the region near the plane of the aperture, especially for guide widths on the order of $\lambda/2$ or less.

Ryan and Rudduck[2] have obtained the radiation patterns of parallel-plate guides with arbitrary geometry by including only the single and double diffraction contributions. Rudduck and Yu[3] have included the third order diffraction contribution and subsequently employed a self-consistent method which includes all higher orders of diffraction from each edge. The radiation patterns obtained by the above analyses have been found to be satisfactory in general. However they do not describe the pattern accurately in the region near the plane of the aperture for small guide widths.

The purpose of the development in this report is to introduce a slope correction term which improves the accuracy in the radiation pattern of the waveguide in this region. The slope correction term is formulated on the basis that the singly diffracted wave incident on the opposite edge is approximated by the superposition of a uniform cylindrical wave and a slope wave. The slope wave is defined as one which has a sinusoidal variation over its wave front. The diffraction of this slope wave is the slope correction term.

The validity of this formulation is demonstrated by the improved accuracy of the radiation pattern analysis for this problem as compared with the previous wedge diffraction analysis. The basis for the comparison is the exact Wiener-Hopf solution[4] for the symmetrical thin-walled parallel-plate waveguide by Wainstein[5] and an accurate, although approximate Fourier transform solution, for the parallel-plate guide mounted in an infinite ground plane by Nussenzveig.[6]

The diffracted field from a conducting wedge due to slope wave incidence is formulated in Chapter II. The slope correction is also checked on an isolated half-plane and a 90° wedge by the surface integration technique[10] in Chapter III. Then the radiation pattern of a parallel-plate waveguide is analyzed in Chapter IV by the wedge diffraction theory in conjunction with this slope correction term.

II. FORMULATION OF SLOPE WAVE DIFFRACTION

In this section the cylindrical slope wave diffraction is formulated as a two dimensional problem. This slope wave has a cylindrical wavefront and a sinusoidal amplitude variation as a function of angle

about the source. The diffraction of the slope wave by a conducting wedge is employed such that the amplitude of the incident wave in the direction of the edge of the conducting wedge is zero. The diffraction of the slope wave is derived from the diffraction of a uniform cylindrical wave by a conducting wedge. For the uniform case, the total field distribution $u(\rho,\varphi)$ at radial distances from the edge which are large compared to that of the line source as shown in Fig. 2 can be expressed as

$$(1) \qquad u(\rho,\varphi) = \frac{e^{-jk\rho}}{\sqrt{\rho}} \left[\left\{ V^*(\rho_o, \psi-\psi_o) + V_B(\rho_o, \psi-\psi_o, n) \right\} \pm \left\{ V^*(\rho_o, \psi+\psi_o) + V_B(\rho_o, \psi+\psi_o, n) \right\} \right] .$$

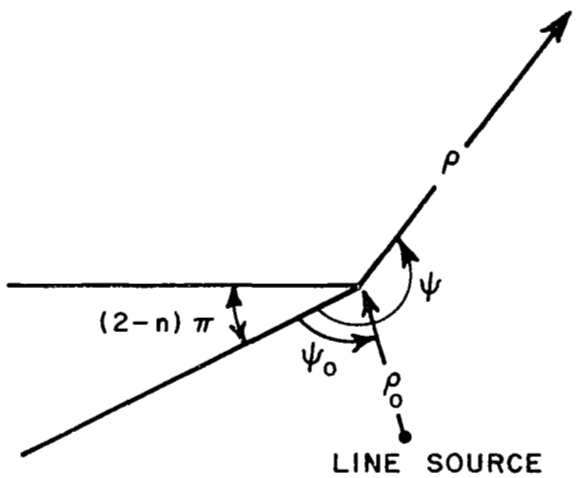

Fig. 2 - Diffraction by a Conducting Wedge

The geometrical optics wave is given by

$$(2) \qquad V^*(\rho,\varphi) = \begin{cases} \exp jk\rho\cos(\varphi + 2\pi nN) \\ \quad \text{if } -\pi < \varphi + 2\pi nN < \pi \text{ for } N = 0, \pm 1, \cdots \\ 0 \qquad \text{otherwise} \end{cases} .$$

The diffracted wave for a conducting wedge of angle $(2-n)\pi$ is given by

$$(3) \qquad V_B(\rho,\varphi,n) = \frac{1}{n} \sum_{m=0}^{\infty} \epsilon_{m/n}\, j^{m/n}\, J_{m/n}(k\rho)\cos\frac{m}{n}\varphi - V^*(\rho,\varphi)$$

where $\epsilon_\alpha = \begin{cases} 1 & \alpha = 0 \\ 2 & \alpha \neq 0 \end{cases}$

and $k = 2\pi/\lambda$ is the free space propagation constant.

The plus or minus sign in Eq. (1) applies for the magnetic field (TM) or electric field (TE) orientated in the z direction, respectively. The plus sign is chosen for the following development since only TM case will be considered here.

The cylindrical slope wave diffraction can be obtained by differentiating the total field with respect to incident angle ψ_o. A similar technique was employed by Keller[7] in which the plane wave diffraction coefficient was differentiated with respected to incident angle α. Ufimtsov[8] has employed similar methods to obtain the secondary diffraction for a strip. The differentiation of the geometrical optics wave with respect to ψ_o is given by

$$(4) \qquad \frac{\partial}{\partial\psi_o} V^*(\rho,\psi \pm \psi_o) = \mp jk\rho \sin(\psi \pm \psi_o)\, V^*(\rho,\psi\pm\psi_o) \quad .$$

The term $\sin\varphi\, V^*(\rho,\varphi)$ is identified as the geometrical optics slope wave V_s^* giving,

$$(5) \qquad V_s^*(\rho,\varphi) = \begin{cases} \sin(\varphi + 2\pi nN)\exp[jk\rho\cos(\varphi + 2\pi nN) \text{ if} \\ \quad -\pi < \varphi + 2\pi nN < \pi \qquad \text{for } N = 0, \pm 1 \cdots \\ 0 \qquad\qquad \text{otherwise.} \end{cases}$$

The slope diffracted wave $V_s(\rho,\varphi,n)$ of a conducting wedge with angle $(2-n)\pi$ can be obtained in a similar manner with the normalization factor $\mp jk\rho$, giving,

$$(6) \qquad V_s(\rho,\varphi,n) = \mp \frac{1}{jk\rho} \frac{\partial}{\partial \psi_o} V_B(\rho,\varphi,n)$$

$$= - \frac{1}{jk\rho n} \sum_{m=0}^{\infty} \frac{m}{n} \epsilon_{m/n} \, j^{m/n} \, J_{m/n}\left(k\rho\right) \sin\left(\frac{m}{n} \varphi\right)$$

$$- V_s^* (\rho,\varphi) \quad .$$

Equation (6) converges rapidly for small values of ρ, i.e., $\rho < \lambda$. However, for large values of ρ, the slope diffracted wave can be obtained in a similar way by using the asymptotic form of the diffracted wave $V_B(\rho,\varphi,n)$. Therefore, the total field distribution U_s at radial distance ρ from the edge of the conducting wedge which is large compared to the distance ρ_o of the slope wave line source is given by

$$(7) \qquad U_s(\rho,\varphi) = \frac{e^{-jk\rho}}{\sqrt{\rho}} \left\{ \left[V_s^* (\rho_o, \psi - \psi_o) + V_s(\rho_o, \psi - \psi_o, n) \right] \right.$$

$$\left. - \left[V_s^* (\rho_o, \psi + \psi_o) + V_s(\rho_o, \psi + \psi_o, n) \right] \right\} \quad .$$

III. PATTERN ANALYSIS FOR A SINGLE EDGE

In this section, the diffraction pattern of a half-plane, i.e., $n = 2$, and a 90° wedge, i.e., $n = 1.5$, due to a nonuniform singly diffracted wave incidence is formulated by use of wedge diffraction in conjunction with the slope correction term. The validity of this formulation is checked numerically by the surface integration technique.[9,10] The geometries for the half-plane and the 90° wedge are shown in Figs. 3 and 4, respectively. The singly diffracted wave from edge 2 will be taken as the source for diffraction from edge 1.

The nonuniform, single diffracted wave from edge 2 is obtained by the diffraction of the plane wave incident on edge 2 from the waveguide giving

$$(8) \qquad H_2^{(1)}(\rho,\theta) = V_B(\rho,\pi - \theta,n) \quad .$$

The angular variation of this wave is obtained by suppressing the factor $\frac{e^{-j(k\rho+\pi/4)}}{\sqrt{2\pi k\rho}}$ in the asymptotic expansion of $V_B(\rho,\varphi,n)$ which is valid for large values of $k\rho(1 + \cos\varphi)$. This gives

$$(9) \qquad R_2^{(1)}(\theta) = \frac{1}{n} \sin\frac{\pi}{n} \Big/ \left(\cos\frac{\pi}{n} - \cos\frac{\pi-\theta}{n}\right) \qquad 0 < \theta \leq \frac{\pi}{2} \quad .$$

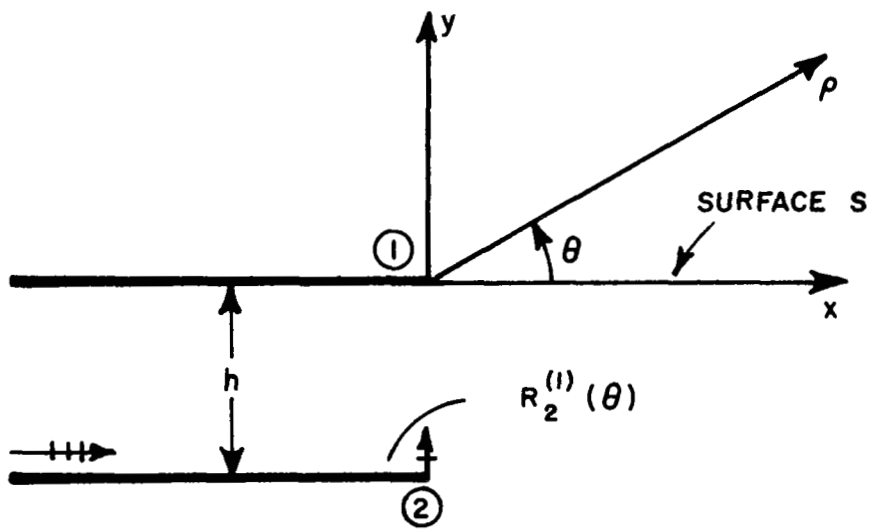

Fig. 3 - Nonuniform Wave Diffraction of a Half-Plane

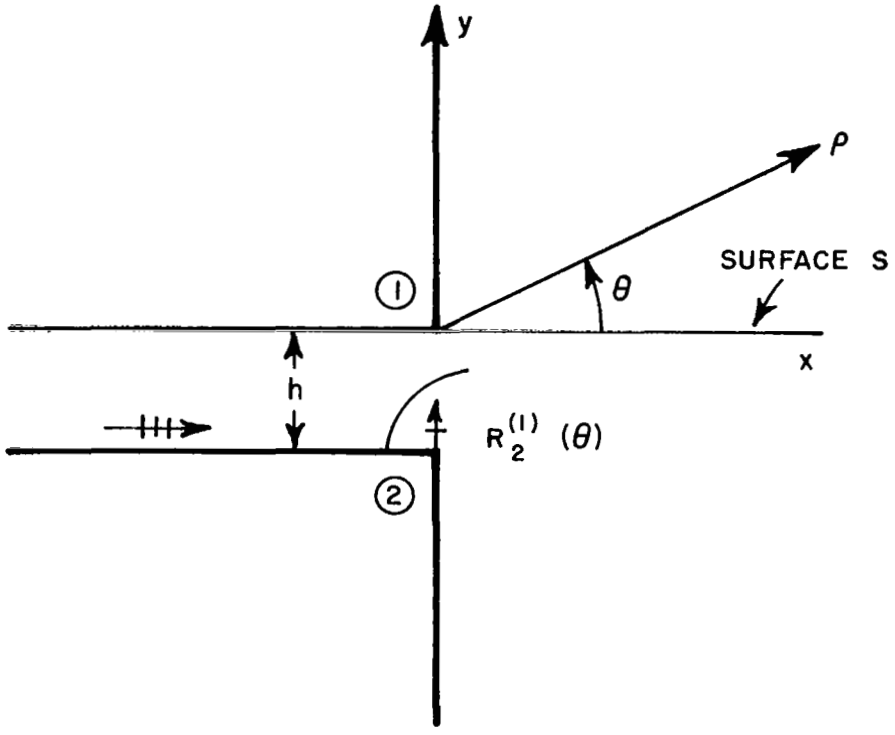

Fig. 4 - Nonuniform Wave Diffraction of a 90° Wedge

The nonuniform cylindrical wave expressed by Eq. (9) can be approximated as a uniform cylindrical wave and a cylindrical slope wave for directions near $\theta = 90°$, giving,

$$R_2^{(1)}(\theta) \approx C_1 + C_2 \sin\left(\frac{\pi}{2} - \theta\right) \tag{10}$$

where C_1 is the magnitude of the uniform cylindrical wave and C_2 is the magnitude of the cylindrical slope wave. Having the factor $\frac{e^{-j\left(k\rho + \frac{\pi}{4}\right)}}{\sqrt{2\pi k\rho}}$ suppressed, the values of C_1 and C_2 are given by

$$C_1 = R_2^{(1)}(\theta)\Big|_{\theta = \frac{\pi}{2}} \tag{11}$$

and

$$C_2 = \frac{-dR_2^{(1)}(\theta)}{d\theta}\Big|_{\theta = \frac{\pi}{2}} \tag{12}$$

Thus the total far field or diffraction pattern due to the singly diffracted wave from edge 2 in Figs. 3 and 4 may be expressed as

$$R_T(\theta) = R_2^{(1)}(\theta) e^{-jkh \sin \theta} + R_d(\theta) + S_d(\theta) \tag{13}$$

in the region $0 < \theta < \pi - WA1$,

where $R_2^{(1)}(\theta)$ is given by Eq. (9). The factor $e^{-jkh \sin \theta}$ refers the phase of the singly diffracted wave from edge 2 to edge 1.

The diffracted field due to the uniform cylindrical wave component is given by

$$R_d(\theta) = C_1\left[V_B\left(h, \theta + \frac{\pi}{2}, n\right) + V_B\left(h, \theta + \frac{3\pi}{2}, n\right)\right] , \tag{14}$$

and the slope correction term is given by

$$S_d(\theta) = C_2\left[V_s\left(h, \theta + \frac{\pi}{2}, n\right) - V_s\left(h, \theta + \frac{3\pi}{2}, n\right)\right] . \tag{15}$$

The magnitude and phase of the diffraction pattern for a half plane due to the nonuniform cylindrical wave located at a distance h away from edge 1 as shown in Fig. 3 are given in Tables I and II for h equal to 0.3 λ and 0.4 λ, respectively. The diffraction pattern without the slope correction term (Eq. 15), which is denoted as double diffraction, is also tabulated as shown. The results for the case of the 90° wedge are given in Tables III and IV.

The diffraction patterns due to the nonuniform singly diffracted waves are compared with calculations by the surface integration technique[9,10] in Figs. 5 - 8 and Tables I - IV. By the surface integration method the far field due to this nonuniform wave is calculated by integration of the field on the surface S shown in Figs. 3 and 4. The field on S was calculated by the wedge diffraction method; that is, the superposition of the singly diffracted fields from edge 2 and the doubly diffracted fields from edge 1 (the latter calculated by assuming uniform cylindrical wave incidence from edge 2).

Slope diffraction is not included on the surface S since its effect in that region is quite small as compared with the incident singly diffracted wave. Furthermore, the approximation of the slope wave diffraction is less accurate away from the direction of the incident slope wave.

The diffraction patterns are plotted in Figs. 7 and 8 for the 90° wedge. It is noted that the patterns calculated by including the slope correction term agree well with those by the surface integration technique. Thus it is seen from these results that the slope correction term improves the accuracy of the wedge diffraction analysis in the region near the shadow boundary of the incident wave.

IV. ANALYSIS OF WAVEGUIDE PATTERNS

In this section the radiation pattern of a TEM mode parallel-plate waveguide as shown in Fig. 9 is analyzed by wedge diffraction theory in conjunction with the slope correction term. The diffraction from the guide aperture is treated by superposing the diffracted waves from each of the edges. The singly diffracted field from each edge is obtained from the plane wave diffraction function $V_B(\rho,\varphi,n)$.[1] The singly diffracted ray $R_1^{(1)}(\theta)$ from edge 1 due to a unit-amplitude plane wave incidence of the TEM mode is obtained from the asymptotic form of $V_B(\rho,\varphi,n)$ as

$$(16) \qquad R_1^{(1)}(\theta) = \frac{1}{n_1} \sin \frac{\pi}{n_1} \left(\frac{1}{\cos \frac{\pi}{n_1} - \cos\left(\frac{\pi+\theta}{n_1}\right)} \right) .$$

Tables I and II

	Theta	Double Diffraction		Slope Correction		Surface Integration	
	In Degrees	Mag.	Phase	Mag.	Phase	Mag.	Phase
Guide Width 0.3 λ	40	1.408	113.2	1.391	112.3	1.400	111.9
	60	0.863	89.6	0.854	86.2	0.882	86.5
	80	0.549	71.9	0.600	65.4	0.611	67.1
	90	0.436	63.9	0.522	57.1	0.521	59.8
	120	0.337	47.8	0.373	41.0	0.360	45.0
	140	0.297	42.1	0.317	35.6	0.307	39.9
	160	0.274	39.0	0.287	33.1	0.271	39.1
Guide Width 0.4 λ	40	1.432	90.6	1.414	90.1	1.419	89.4
	60	0.876	59.7	0.869	57.0	0.882	57.0
	80	0.545	37.7	0.583	31.8	0.596	33.1
	90	0.424	28.4	0.498	22.2	0.498	24.4
	120	0.312	10.2	0.339	4.2	0.329	8.8
	140	0.268	4.1	0.282	-1.4	0.274	2.0
	160	0.245	1.0	0.253	-3.9	0.248	-0.1

Tables III and IV

Theta	Double Diffraction		Slope Correction		Surface Integration	
In Degrees	Mag.	Phase	Mag.	Phase	Mag.	Phase
Guide Width 0.31831 λ						
20	2.683	139.3	2.654	139.2	2.679	139.1
40	1.323	103.5	1.293	101.5	1.326	101.6
60	0.896	77.6	0.909	71.8	0.941	73.0
80	0.692	64.0	0.790	55.3	0.809	57.6
90	0.626	62.0	0.779	53.2	0.795	55.6
Guide Width 0.44563 λ						
20	2.657	124.3	2.639	124.5	2.651	124.3
40	1.302	74.4	1.269	73.4	1.293	72.9
60	0.885	38.0	0.879	33.5	0.906	33.9
80	0.683	19.0	0.757	11.4	0.773	12.6
90	0.618	16.4	0.745	8.6	0.758	10.0

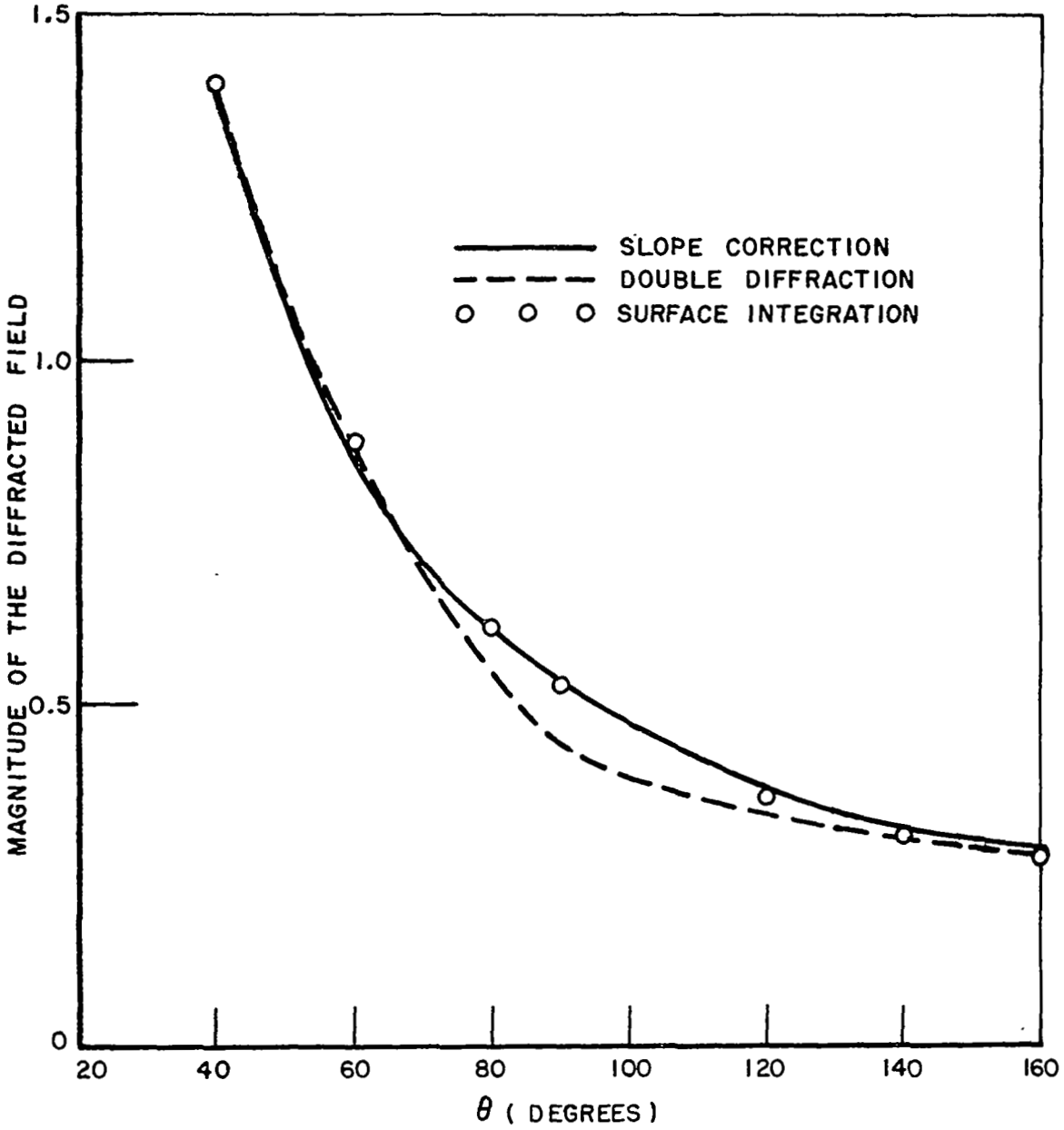

Fig. 5 - Diffraction Pattern of a Half-Plane ($h/\lambda = 0.3$)

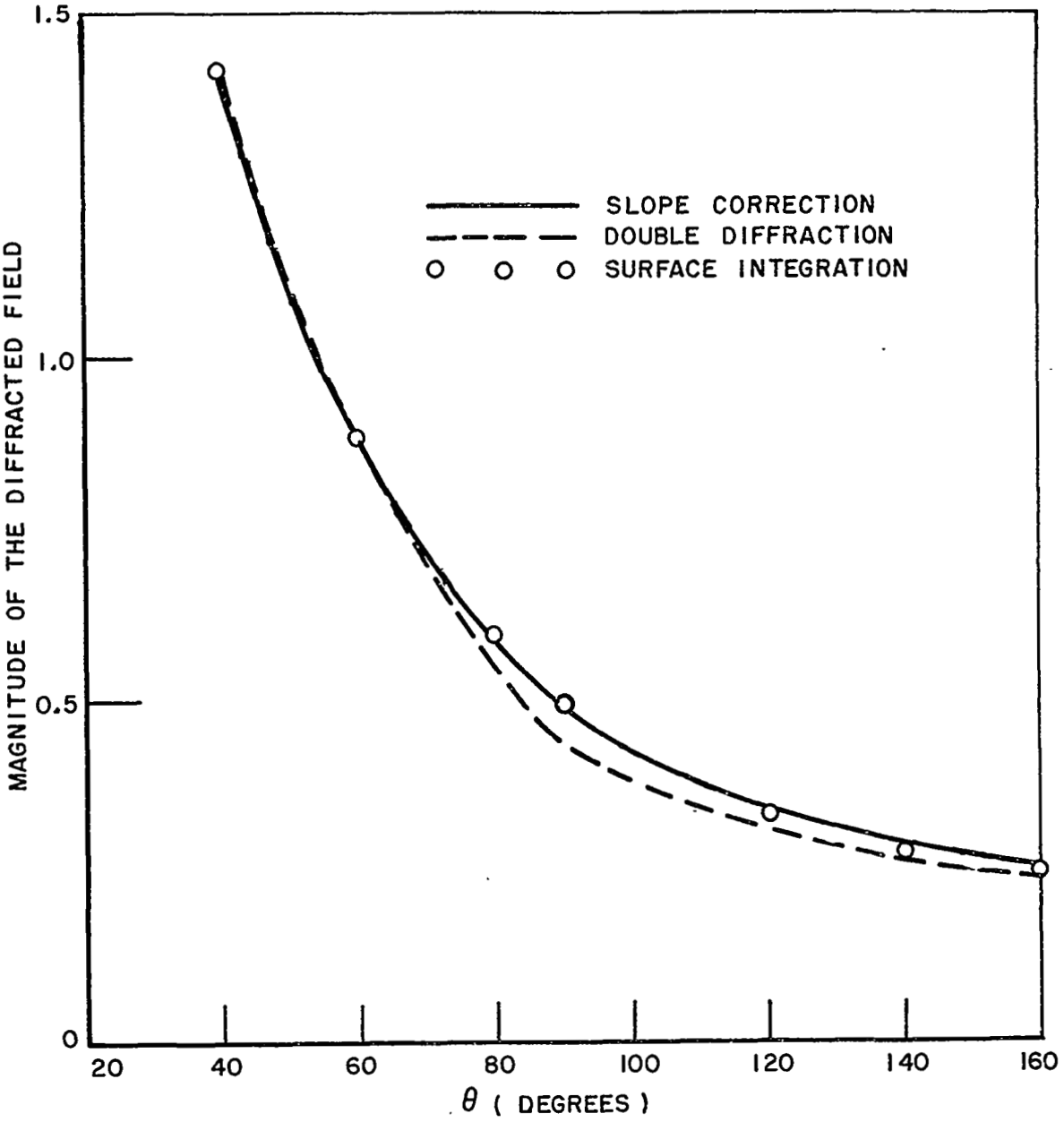

Fig. 6 - Diffraction Pattern of a Half-Plane ($h/\lambda = 0.4$)

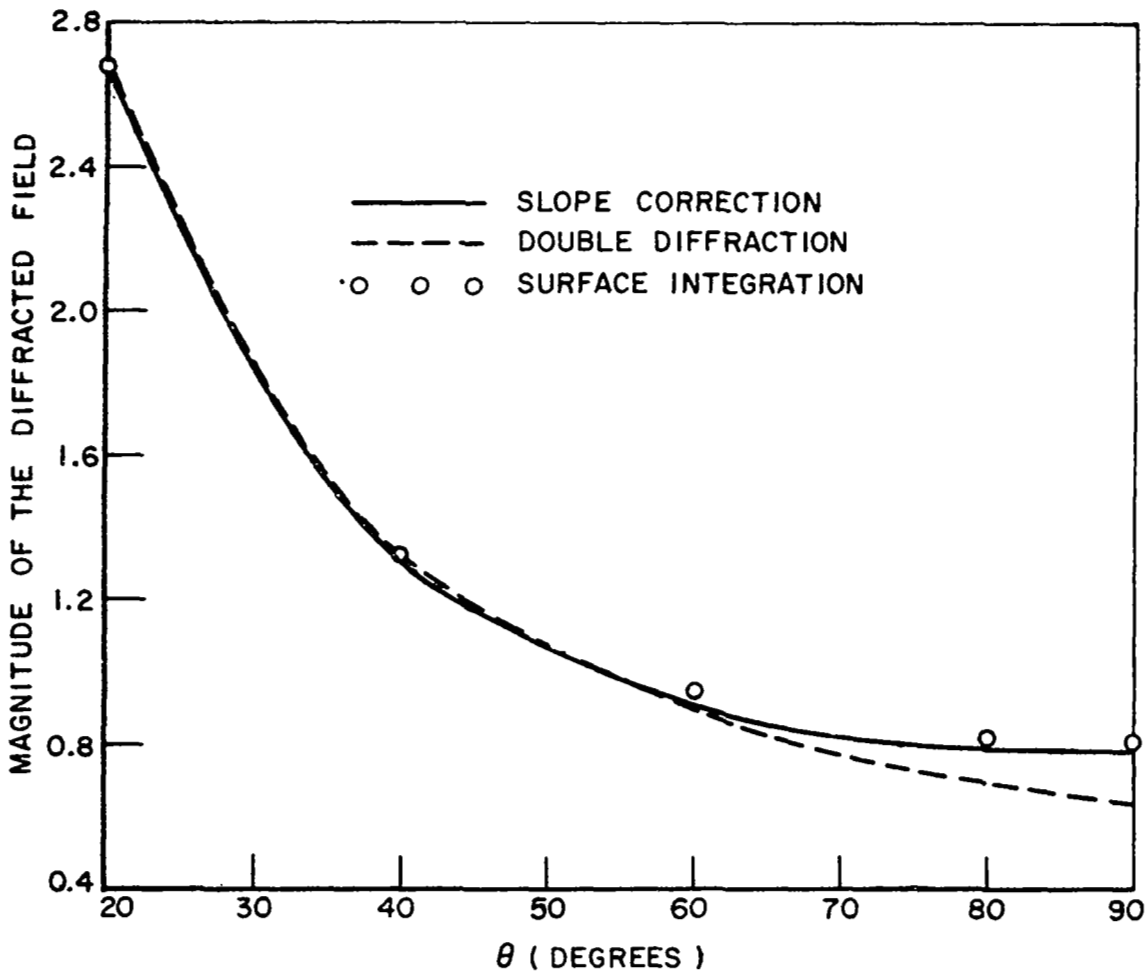

Fig. 7 - Diffraction Pattern of a 90° Wedge ($h/\lambda = 0.3183$)

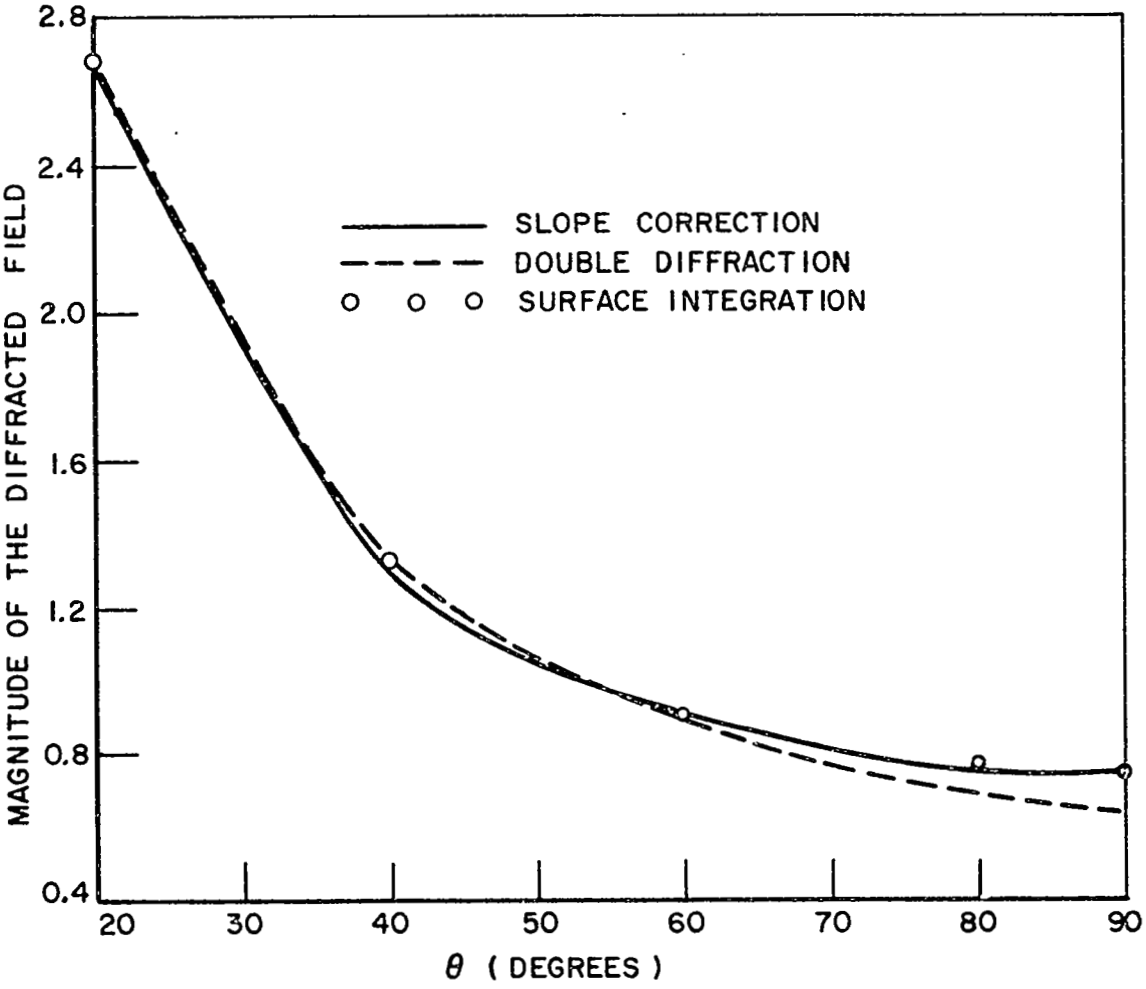

Fig. 8 - Diffraction Pattern of a 90° Wedge ($h/\lambda = 0.4456$)

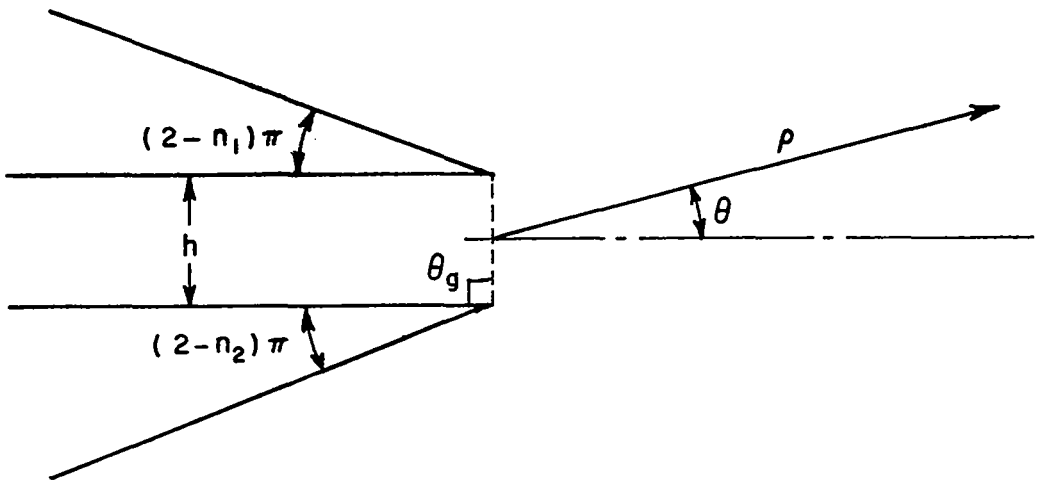

Fig. 9 - Geometry of the Parallel-Plate Guide

The factor $\frac{e^{-j(k\rho + \frac{\pi}{4})}}{\sqrt{2\pi k\rho}}$ is suppressed in Eq. (16) because only angular variations are of interest. The subscript 1 denotes edge 1 and the superscript (1) denotes the first order diffraction due to the incident plane wave. Similarly, the singly diffracted ray from edge 2 is obtained as

$$(17) \qquad R_2^{(1)}(\theta) = \frac{1}{n_2} \sin \frac{\pi}{n_2} \left(\frac{1}{\cos \frac{\pi}{n_2} - \cos\left(\frac{\pi-\theta}{n_2}\right)} \right)$$

The direction $\theta = 0°$ corresponds to the direction of the geometrical optics rays. It is noted that the individual rays $R_1^{(1)}(\theta)$ and $R_2^{(1)}(\theta)$ diverge at $\theta = 0°$, yet the sum of $R_1^{(1)}(\theta)$ and $R_2^{(1)}(\theta)$ with the same phase reference expresses the effect of the geometrical optics rays as given by

$$(18) \qquad R_T^{(1)}(0) = \lim_{\theta \to 0°} \left[R_1^{(1)}(\theta)\, e^{+\frac{jkh}{2}\sin\theta} + R_2^{(1)}(\theta)\, e^{-\frac{jkh}{2}\sin\theta} \right]$$

$$= jkh - \frac{1}{2n_1} \cot \frac{\pi}{n_1} - \frac{1}{2n_2} \cot \frac{\pi}{n_2}$$

where $e^{\pm (jkh/2) \sin \theta}$ refers the phase to the center of the guide aperture. The singly diffracted wave from edge 1 $R_1^{(1)}(\theta)$, illuminates edge 2 giving rise to the doubly diffracted wave $R_{2T}^{(2)}\theta)$, and $R_2^{(1)}(\theta)$ causes $R_{1T}^{(2)}(\theta)$ in a similar manner.

The formulation of the doubly diffracted wave was discussed in the previous section. Employing the notations as shown in Table V, the total doubly diffracted wave from edge 1 is given by

$$R_{1T}^{(2)}(\theta) = R_1^{(2)}(\theta) + S_1^{(2)}(\theta) \tag{19}$$

where $R_1^{(2)}(\theta)$ is the doubly diffracted wave due to the uniform component and $S_1^{(2)}(\theta)$ is due to the slope component of the incident singly diffracted wave from edge 2. The uniform component of the diffraction is given by

$$R_1^{(2)}(\theta) = R_{2G}^{(1)}\left[V_B\left(h,\theta + \frac{\pi}{2},n_1\right) + V_B\left(h,\theta + \frac{3\pi}{2},n_1\right)\right] \tag{20}$$

where

$$R_{2G}^{(1)} = R_2^{(1)}(\pi - \theta g) = R_2^{(1)}\left(\frac{\pi}{2}\right) \tag{21}$$

is the value of the singly diffracted ray from edge 2 in the direction of edge 1. The slope diffraction component is given by

$$S_1^{(2)}(\theta) = S_{2G}^{(1)}\left[V_S\left(h,\theta + \frac{\pi}{2},n_1\right) - V_S\left(h,\theta + \frac{3\pi}{2},n_1\right)\right] \tag{22}$$

where

$$S_{2G}^{(1)} = \frac{-\partial R_2^{(1)}(\theta)}{\partial \theta}\Big|_{\theta = \pi - \theta g = \frac{\pi}{2}} \tag{23}$$

is the slope of the singly diffracted wave in the direction of edge 1.

The total doubly diffracted wave from edge 2 is obtained in a similar way as

$$R_{2T}^{(2)}(\theta) = R_2^{(2)}(\theta) + S_2^{(2)}(\theta) \tag{24}$$

Table V

Notation for Rays

Ray	Description	Source
$R_1^{(1)}(\theta)$	Singly diffracted ray from edge 1	Incident plane wave
$R_2^{(1)}(\theta)$	Singly diffracted ray from edge 2	
$R_{1G}^{(1)} = R_1^{(1)}(-\theta g), \quad S_{1G}^{(1)} = \frac{\partial R_1^{(1)}(\theta)}{\partial \theta}\Big\|_{\theta = -\theta g}$		
$R_{2G}^{(1)} = R_2^{(1)}(\pi - \theta g), \quad S_{2G}^{(1)} = \frac{-\partial R_2^{(1)}(\theta)}{\partial \theta}\Big\|_{\theta = \pi - \theta g}$		
$R_1^{(2)}(\theta)$	Doubly diffracted ray from edge 1 due to uniform component	$R_{2G}^{(1)}$
$S_1^{(2)}(\theta)$	Second order slope diffracted wave from edge 1	$S_{2G}^{(1)}$
$R_2^{(2)}(\theta)$	Doubly diffracted ray from edge 2 due to uniform component	$R_{1G}^{(1)}$
$S_2^{(2)}(\theta)$	Second order slope diffracted wave from edge 2	$S_{1G}^{(1)}$
$R_{1T}^{(2)}(\theta) = R_1^{(2)}(\theta) + S_1^{(2)}(\theta)$		
$R_{2T}^{(2)}(\theta) = R_2^{(2)}(\theta) + S_2^{(2)}(\theta)$		

where

$$R_2^{(2)}(\theta) = R_{1G}^{(1)}\left[V_B\left(h,\frac{\pi}{2} - \theta,n_2\right) + V_B\left(h,\frac{3\pi}{2} - \theta,n_2\right)\right] \tag{25}$$

$$S_2^{(2)}(\theta) = S_{1G}^{(1)}\left[V_S\left(h,\frac{\pi}{2} - \theta,n_2\right) - V_S\left(h,\frac{3\pi}{2} - \theta,n_2\right)\right] . \tag{26}$$

Therefore, the total diffracted wave from the aperture may be expressed as the superposition of the total diffracted rays from edges 1 and 2, giving

$$\begin{aligned} R(\theta) = &\left(R_1^{(1)}(\theta) + R_{1T}^{(2)}(\theta)\right)e^{\frac{jkh}{2}\sin\theta} \\ &+ \left(R_2^{(1)}(\theta) + R_{2T}^{(2)}(\theta)\right)e^{\frac{-jkh}{2}\sin\theta} \end{aligned} \tag{27}$$

Each term in Eq. (27) contributes to the radiation pattern of the parallel-plate waveguide only in certain regions as given in Table VI.

Several terminologies such as double diffraction, continuous-double and slope correction have been introduced in computing the radiation pattern. This is done to classify the different contributions of rays in appropriate regions as shown in Table VI. The radiation pattern denoted as double diffraction includes the singly and doubly diffracted rays from both edges. In the continuous-double result only the doubly diffracted rays from the nearest edge are included. This result thus gives a continuous pattern because the doubly diffracted rays from the furthest edge are shadowed by the nearest waveguide wall. The slope diffracted rays from the nearest edge are added to the continuous-double to form the slope correction result.

The TEM radiation pattern of the symmetrical parallel-plate guide (i.e., $n_1=n_2=n$) was calculated for various wedge angles. However, the patterns for the thin-walled and ground-plane guides are treated more extensively in the following sections.

A. Thin-Walled Guide

The radiation patterns for the thin-walled case are compared in Figs. 10 to 14 for the three different formulations i.e., double diffraction, continuous-double and slope correction. Results are given for five values of guide width h, ranging from 0.1 to 0.5 λ. In each case the radiation pattern is normalized to unity at $\theta = 0°$ with normalization factor kh. The exact radiation pattern as calculated by the Wiener-Hopf method[4] is also plotted as shown for comparison. The magnitude and phase of the radiation patterns as calculated by the

Table VI

	$-180° + WA2 < \theta < -90°$	$-90° < \theta < 0°$	$0° < \theta < 90°$	$90° < \theta < 180°-WA1$	
Double Diffraction	$R_2^{(1)}(\theta)$, $R_2^{(2)}(\theta)$	$R_1^{(1)}(\theta)$, $R_1^{(2)}(\theta)$ $R_2^{(1)}(\theta)$, $R_2^{(2)}(\theta)$	$R_1^{(1)}(\theta)$, $R_1^{(2)}(\theta)$ $R_2^{(1)}(\theta)$, $R_2^{(2)}(\theta)$	$R_1^{(1)}(\theta)$, $R_1^{(2)}(\theta)$	Edge 1 Edge 2
Continuous Double	$R_2^{(1)}(\theta)$, $R_2^{(2)}(\theta)$	$R_1^{(1)}(\theta)$ $R_2^{(1)}(\theta)$, $R_2^{(2)}(\theta)$	$R_1^{(1)}(\theta)$, $R_1^{(2)}(\theta)$ $R_2^{(1)}(\theta)$	$R_1^{(1)}(\theta)$, $R_1^{(2)}(\theta)$	Edge 1 Edge 2
Slope Correction	$R_2^{(1)}(\theta)$, $R_2^{(2)}(\theta)$, $S_2^{(2)}(\theta)$	$R_1^{(1)}(\theta)$ $R_2^{(1)}(\theta)$, $R_2^{(2)}(\theta)$, $S_2^{(2)}(\theta)$	$R_1^{(1)}(\theta)$, $R_1^{(2)}(\theta)$, $S_1^{(2)}(\theta)$ $R_2^{(1)}(\theta)$	$R_1^{(1)}(\theta)$, $R_1^{(2)}(\theta)$, $S_1^{(2)}(\theta)$	Edge 1 Edge 2

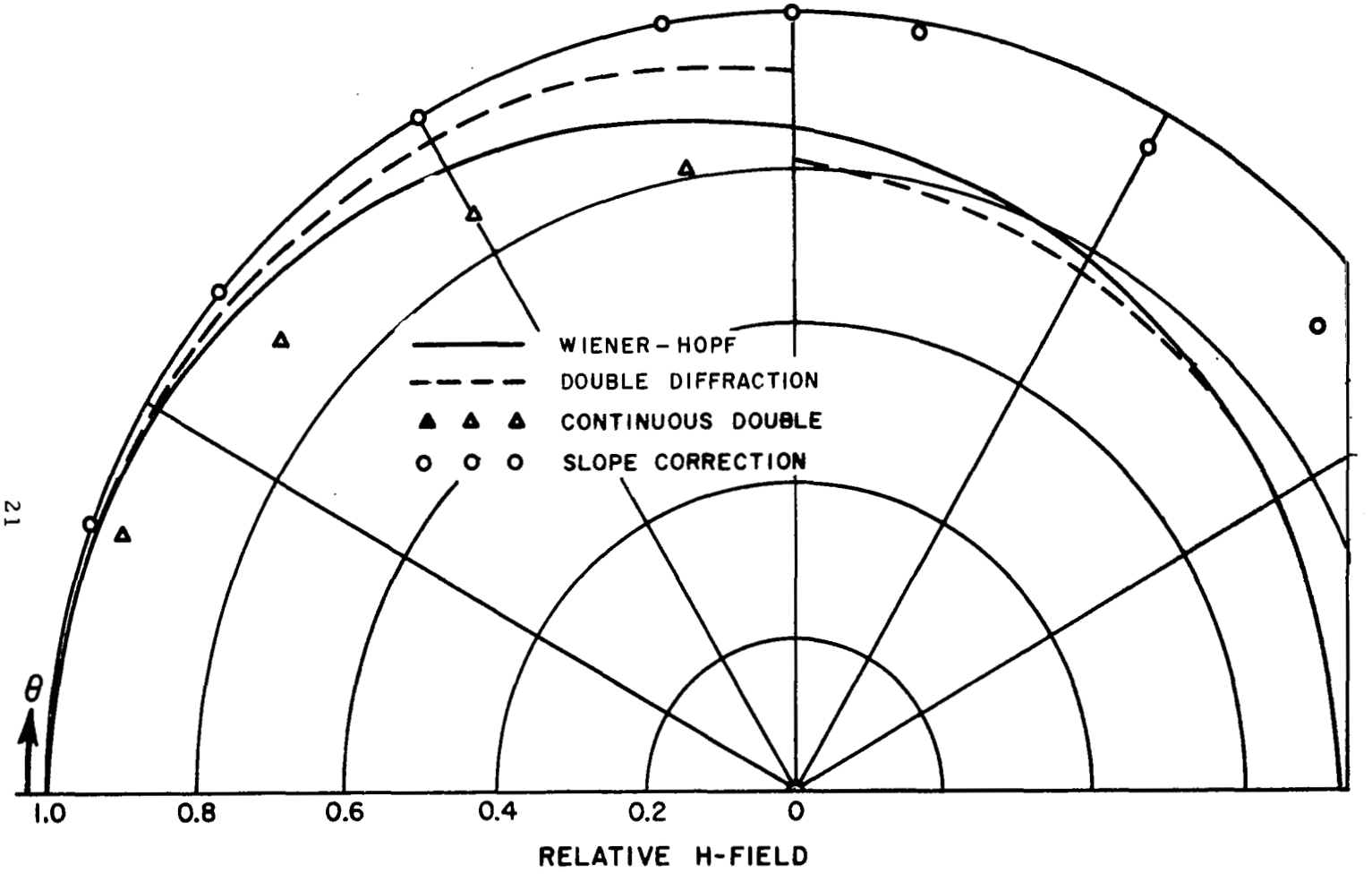

Fig. 10 - Radiation Pattern for TEM Guide ($n = 2$, $h/\lambda = 0.1$)

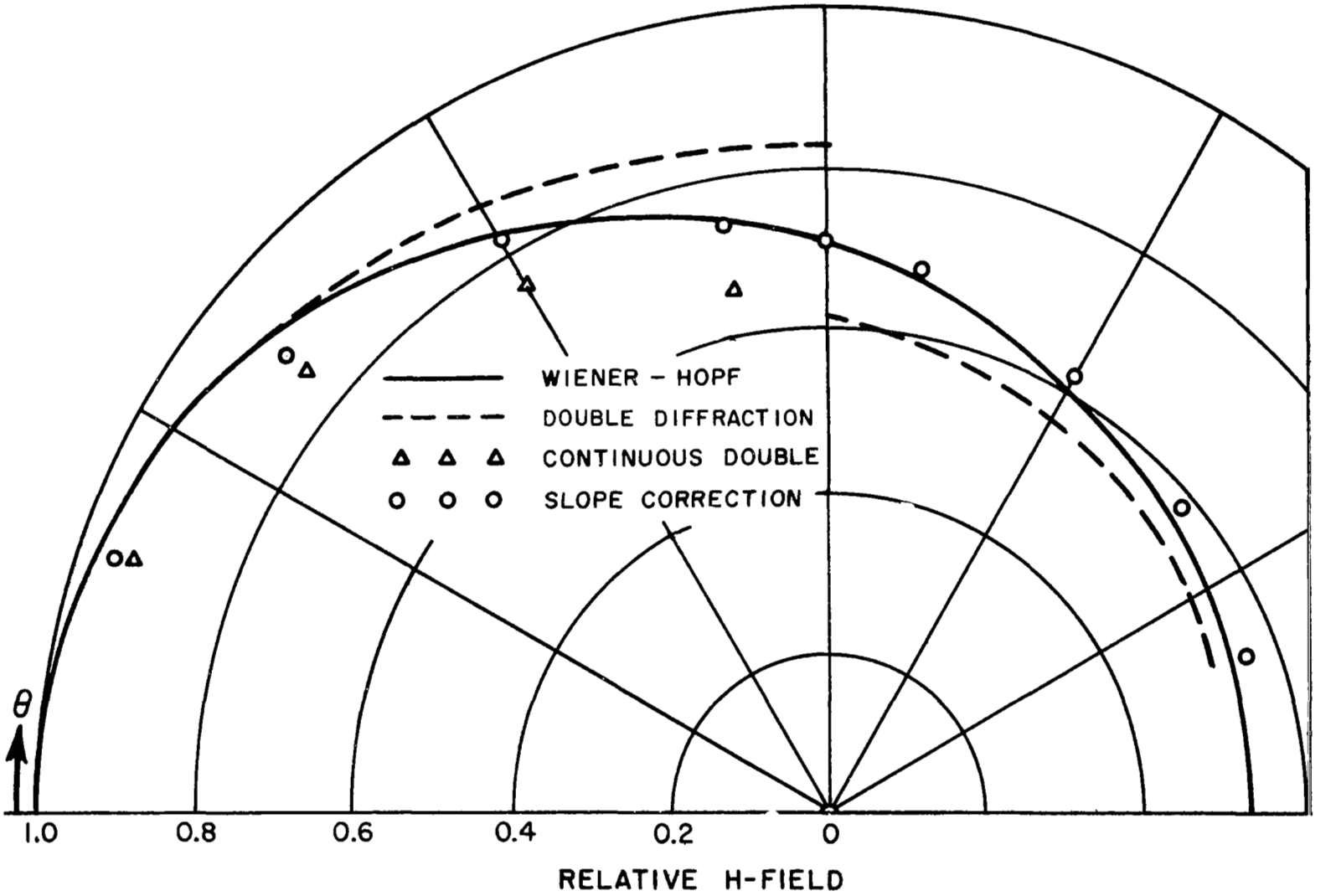

Fig. 11 - Radiation Pattern for TEM Guide ($n = 2$, $h/\lambda = 0.2$)

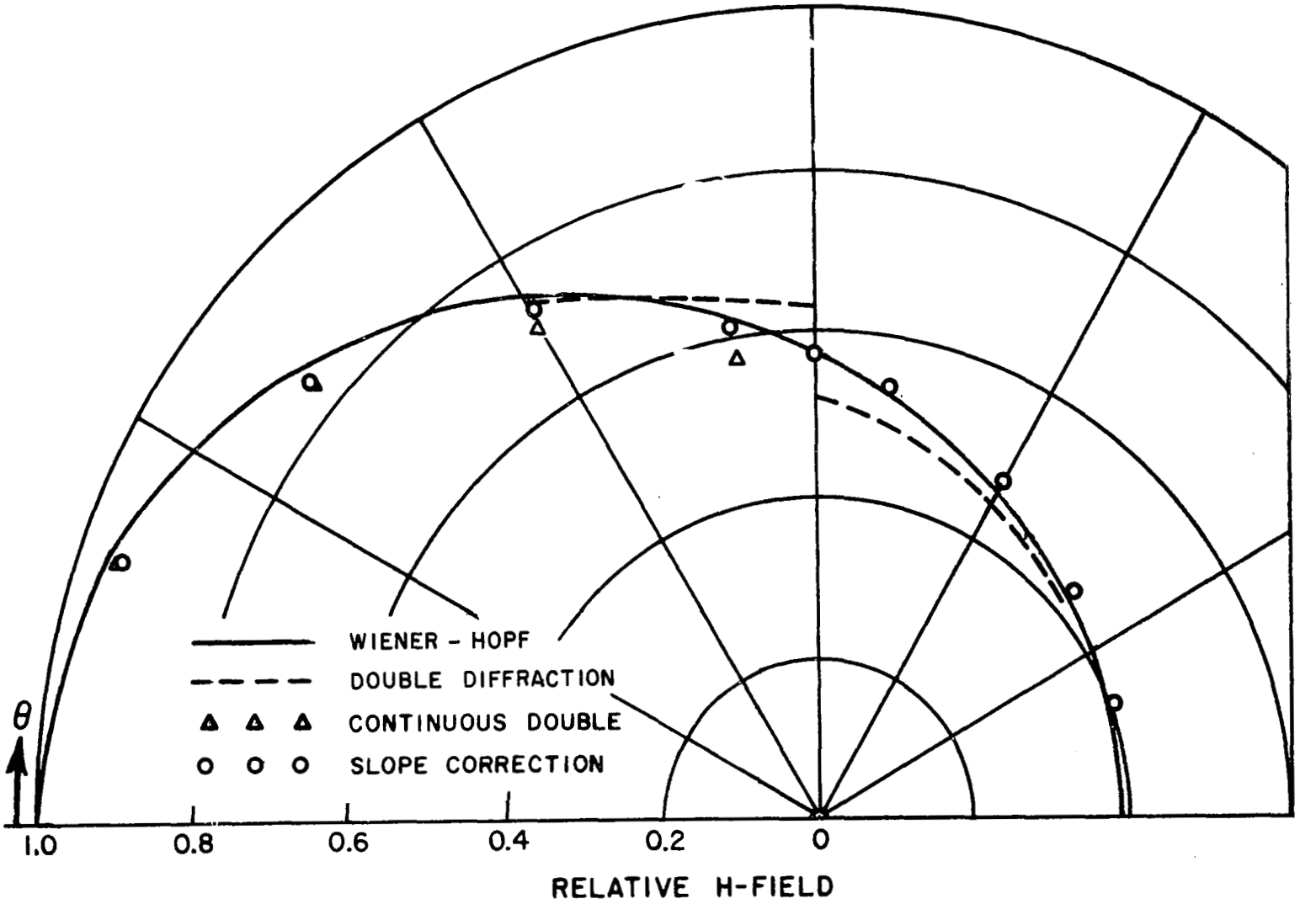

Fig. 12 Radiation Pattern for TEM Guide ($n = 2$, $h/\lambda = 0.3$)

Table VII

$h = 0.3 \lambda$

Theta In Degrees	Weiner Hopf	Double Diffraction	Continuous Double	Slope Correction
1.0	1.0	1.0	1.0	1.0
	90	90	90	90
20	0.964	0.961	0.947	0.948
	89.5	89.3	90.3	89.9
40	0.868	0.859	0.834	0.844
	89.6	87.0	89.7	88.7
60	0.746	0.737	0.703	0.724
	85.5	81.9	87.3	85.9
80	0.629	0.648	0.574	0.617
	80.9	72.9	82.0	81.1
90	0.578	0.520	0.520	0.575
	77.5	77.5	77.5	77.9
100	0.534	0.493	0.493	0.537
	73.2	74.3	74.4	73.8
120	0.466	0.446	0.446	0.474
	62.0	64.0	64.0	62.6
140	0.422	0.413	0.413	0.430
	47.4	49.5	49.5	47.9
160	0.397	0.393	0.393	0.406
	29.8	32.0	32.0	0.3
180	0.390	---	---	---
	---	---	---	---

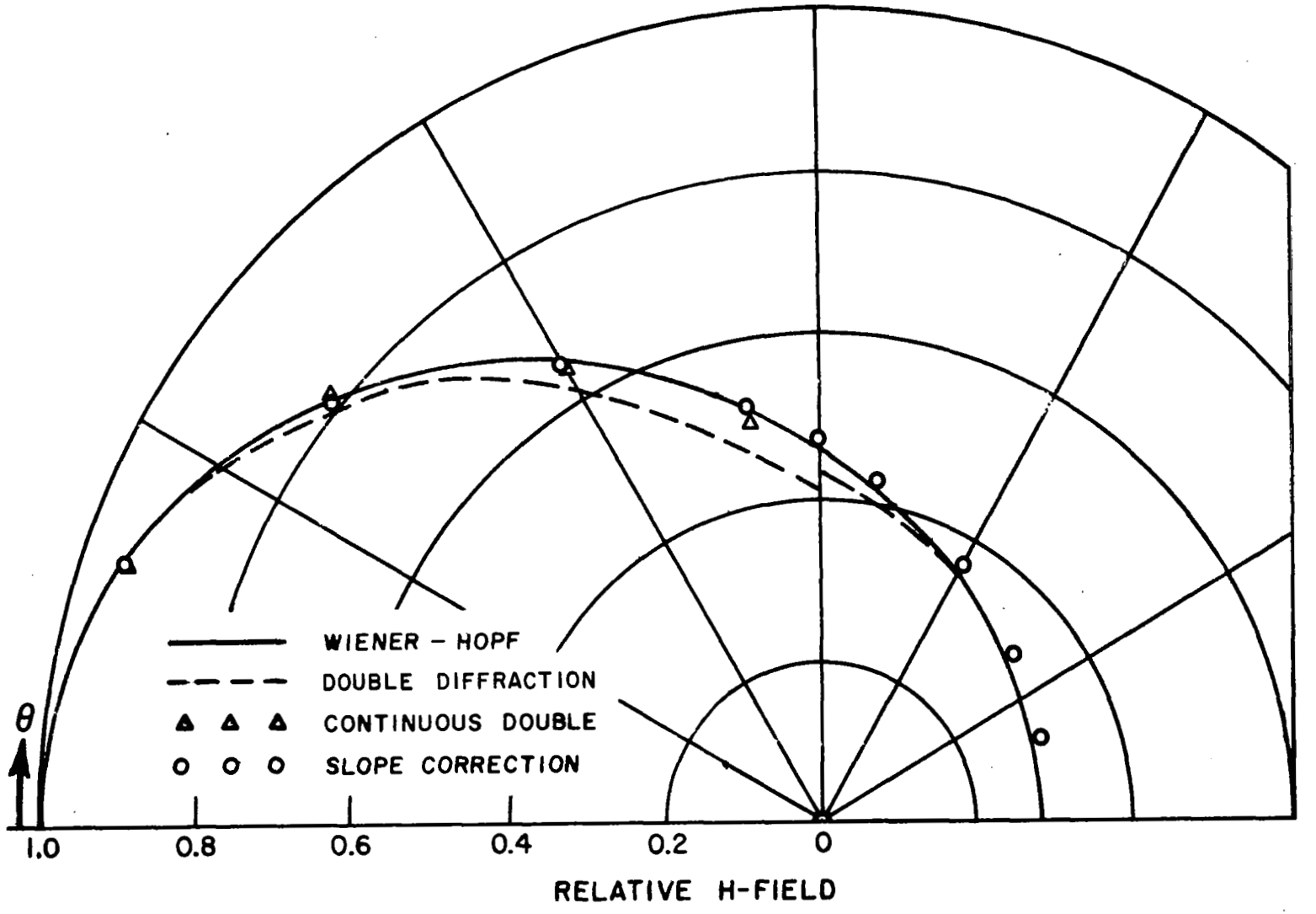

Fig. 13 - Radiation Pattern for TE$_{1}$ Guide ($n = 2$, $h/\lambda = 0.4$)

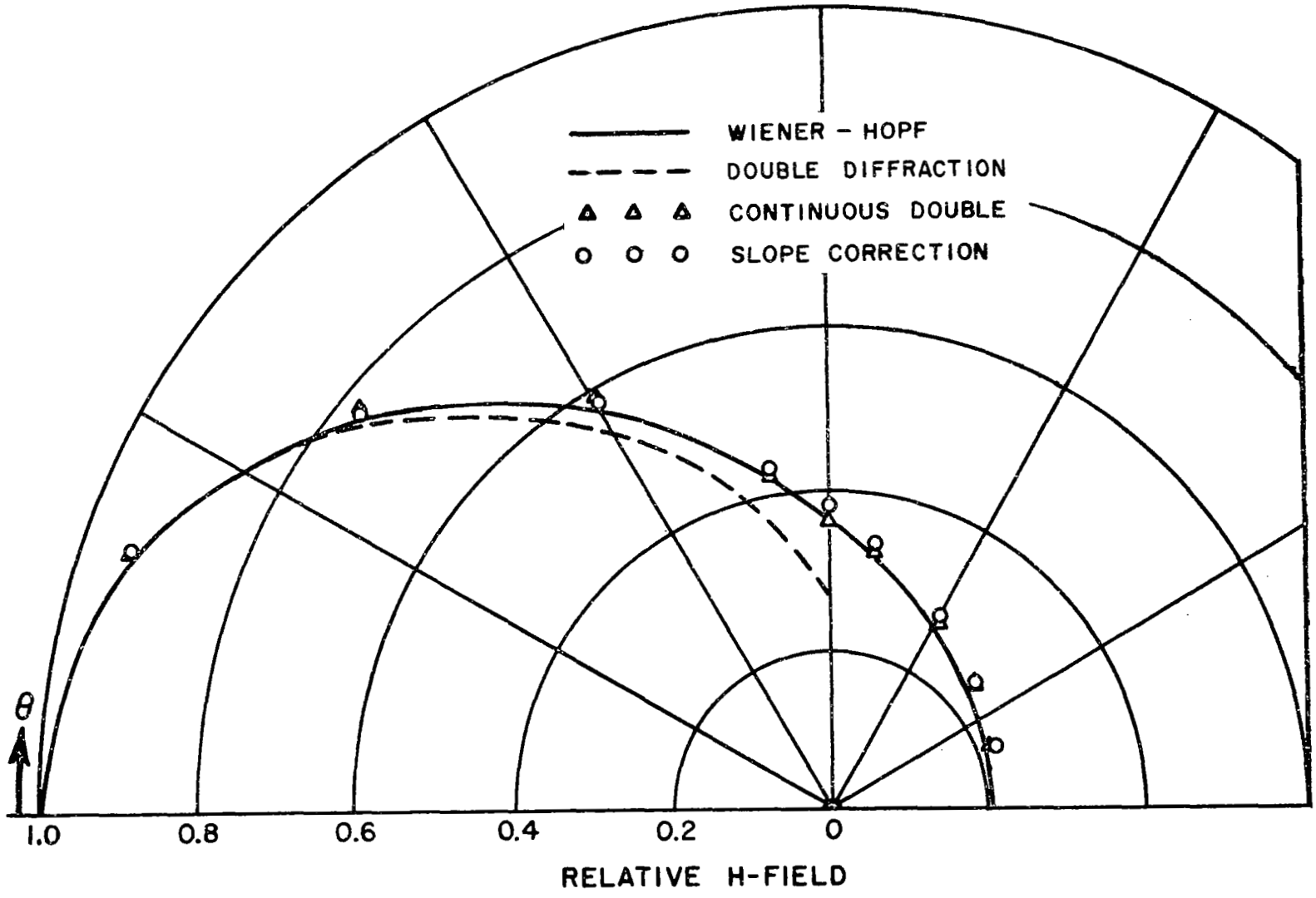

Fig. 14 - Radiation Pattern for TEM Guide ($n = 2$, $h/\lambda = 0.5$)

different methods for a guide width h = 0.3 λ in Table VII.

It is to be noted that the radiation pattern calculated by the Slope Correction method for the case h = 0.1 λ does not agree well with the exact solution. This is not surprising because it is beyond the limit of this formulation (the value of the guide width h is too small to use this technique which is basically a high frequency approximation). However, for guide width h greater than 0.2 λ, it is evident that the slope correction does improve the accuracy of the radiation pattern in the region near the plane of the guide aperture, i.e., $60° < \theta < 120°$.

The effect of slope correction vanishes as the guide width increases. Hence, the radiation pattern calculated by the continuous-double formulation agrees well with the exact solution for guide widths greater than 0.5 λ. The radiation pattern calculated by the double diffraction method is discontinuous at $\theta = 90°$, since the doubly diffracted wave from edge 2, $R_2^{(2)}(\theta)$, is shadowed for $\theta > 90°$ by waveguide wall #1.

Ryan and Rudduck[2] have discussed the contributions to the radiation pattern calculated by the double diffraction method due to each component of the diffracted waves in the different regions.

B. Ground Plane Guide

The radiation patterns of the parallel-plate waveguide mounted in an infinite ground plane are shown in Figs. 15 to 22 for several values of guide width ranging from 0.2 to 0.9 λ. The radiation pattern of this geometry has also been analyzed by Nussenzveig[6] by employing higher order modes in a Fourier transform solution as shown in the Appendix. The higher order modes are actually evanescent modes which do perturb the fields in the aperture of the waveguide. Do Amaral and Vidal[11] have obtained the coefficients of these higher order modes for guide widths up to 0.6 λ. Patterns obtained using the Fourier transform approach are given in the figures.

It has been shown that the on-axis field i.e., $\theta = 0°$, is accurately approximated by merely including the singly and doubly diffracted fields from both edges.[12] The normalization factor for this geometry is given by

$$R_1^{(1)}(0) + R_2^{(1)}(0) + R_1^{(2)}(0) + R_2^{(2)}(0) \quad . \tag{28}$$

The radiation patterns calculated by the double diffraction, continuous-double and slope correction are all normalized with respect to Eq. (28). The magnitudes and the phases of the normalized patterns are tabulated in Table VIII for a guide width h = 0.3183 λ.

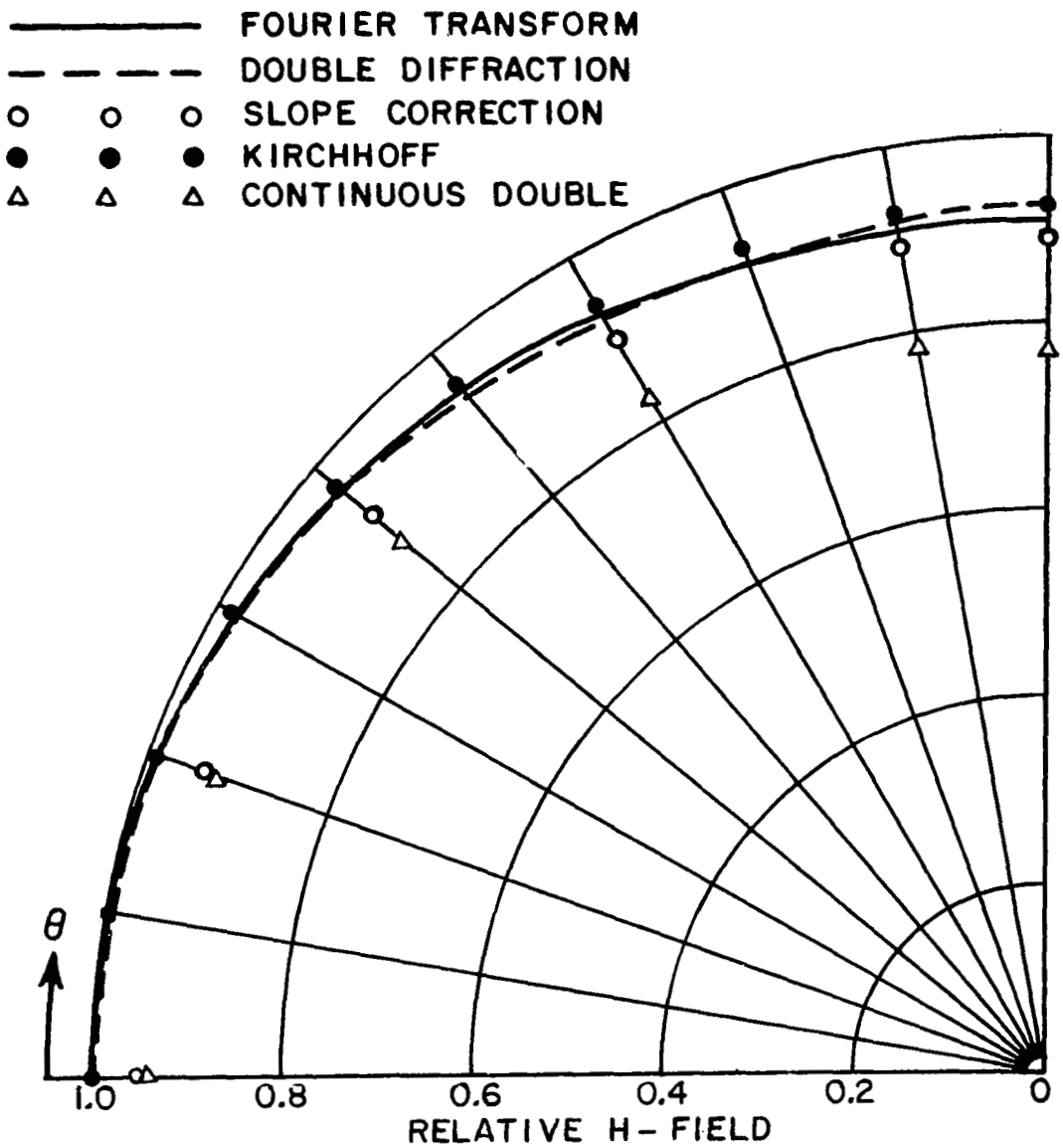

Fig. 15 - Radiation Pattern for TEM Guide ($n = 1.5$, $h/\lambda = 0.2228$)

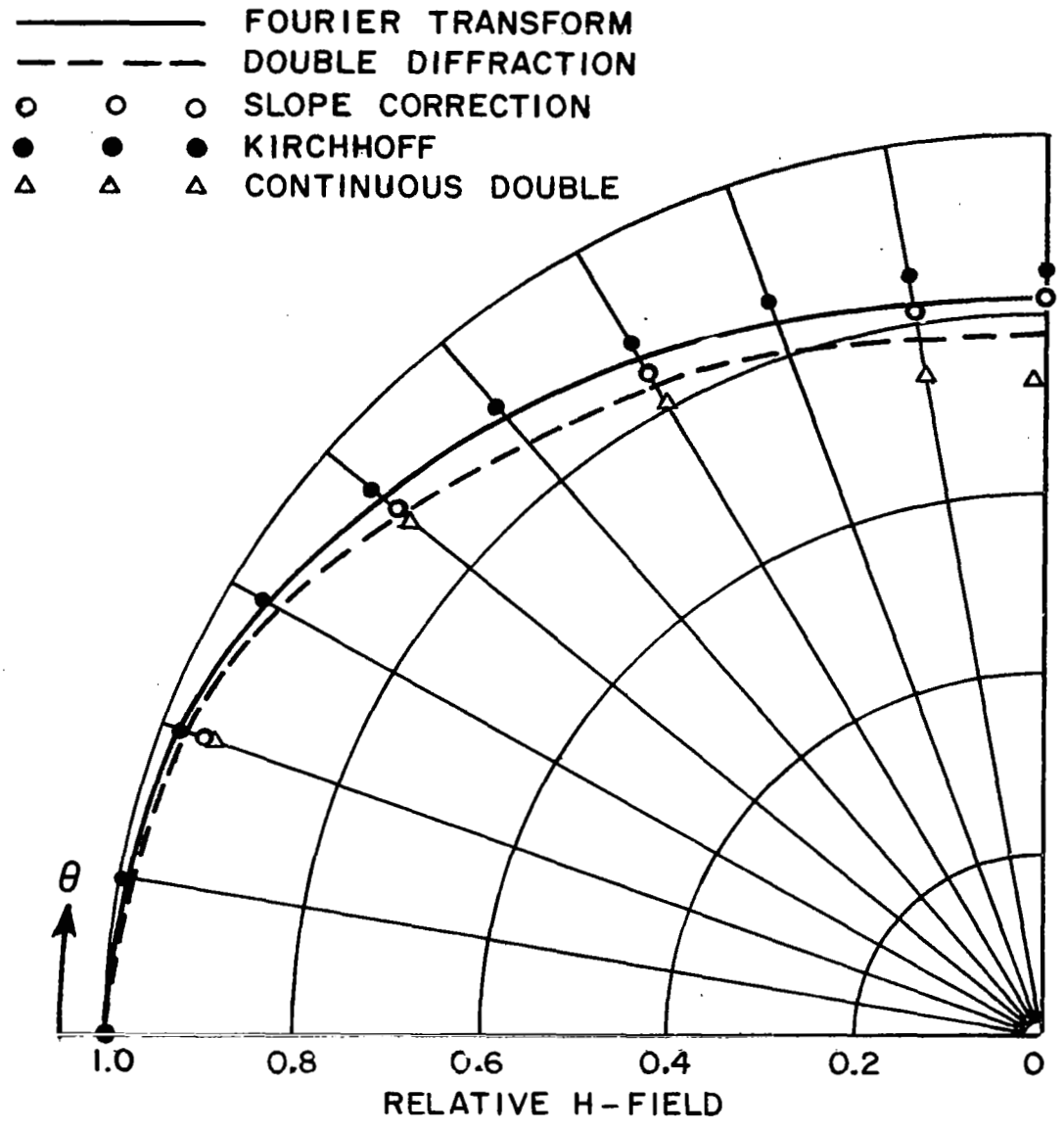

Fig. 16 - Radiation Pattern for TEM Guide ($n = 1.5$, $h/\lambda = 0.3183$)

Table VIII

$h/\lambda = 0.3183$

Theta In Degrees	Kirchhoff	Fourier Transform	Double Diffraction	Continuous-Double	Slope Correction
1.0	1.0	1.0	1.0	0.972	0.969
		75.68	75.78	77.43	77.12
20	0.981	0.977	0.973	0.949	0.949
		75.78	75.76	78.24	77.41
40	0.933	0.919	0.903	0.885	0.897
		76.04	75.49	79.25	77.72
60	0.880	0.857	0.825	0.807	0.841
		76.36	74.43	79.78	78.01
80	0.846	0.817	0.778	0.742	0.809
		76.58	71.73	79.29	78.27
90	0.841	0.811	0.776	0.719	0.805
		76.61	70.0	78.18	78.33

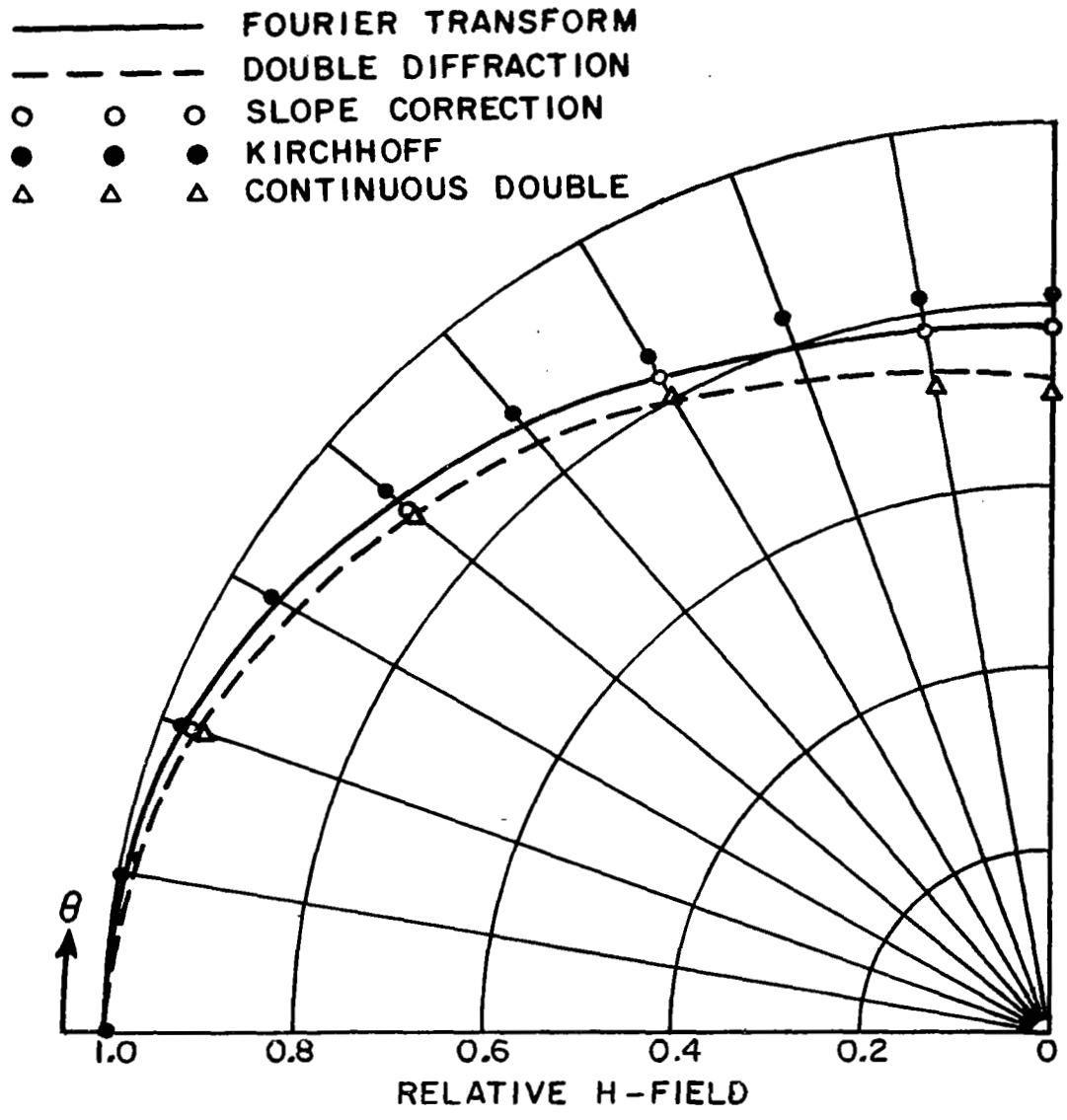

Fig. 17 - Radiation Pattern for TEM Guide ($n = 1.5$, $h/\lambda = 0.3502$)

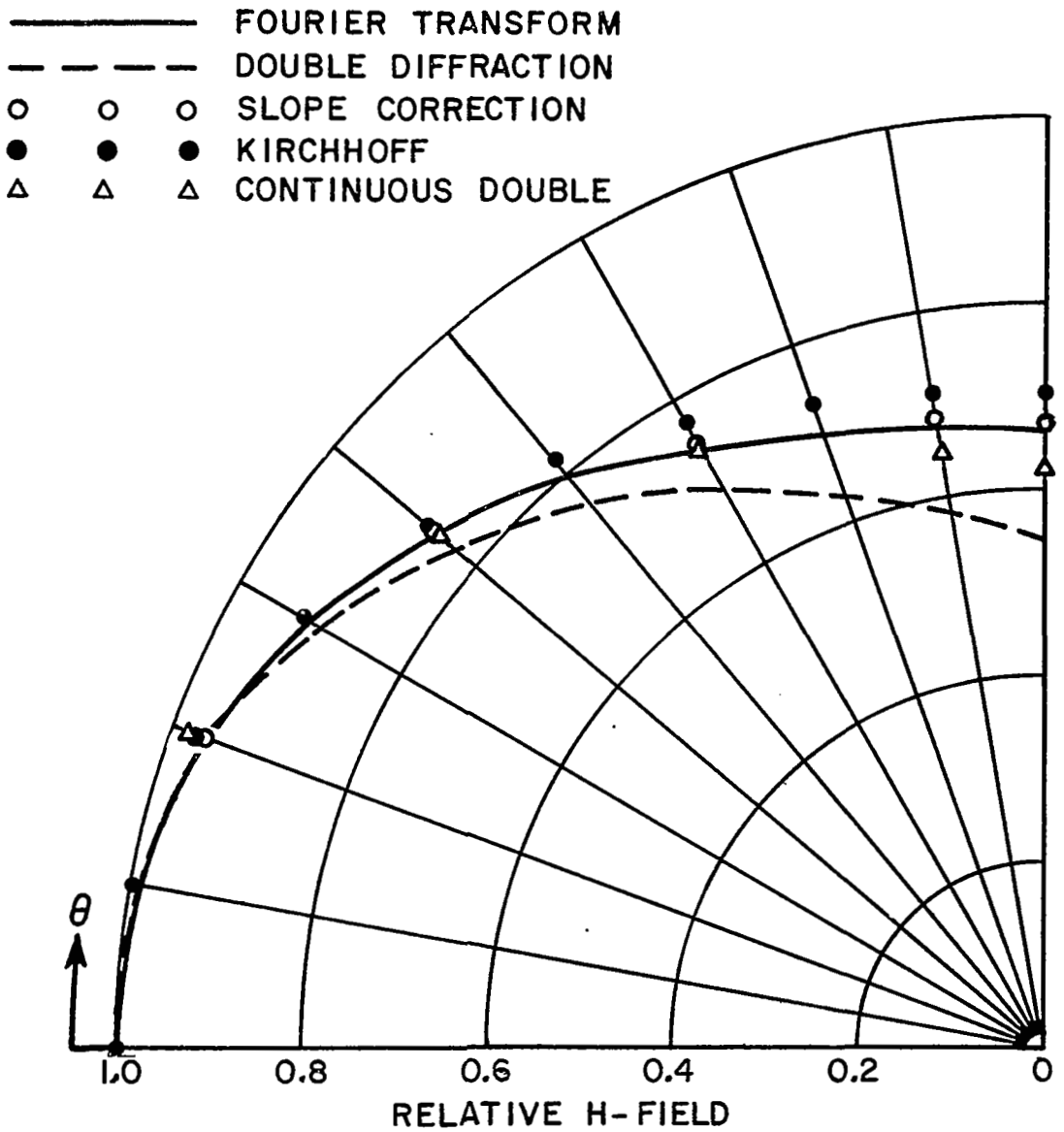

Fig. 18 - Radiation Pattern for TEM Guide ($n = 1.5$, $h/\lambda = 0.4456$)

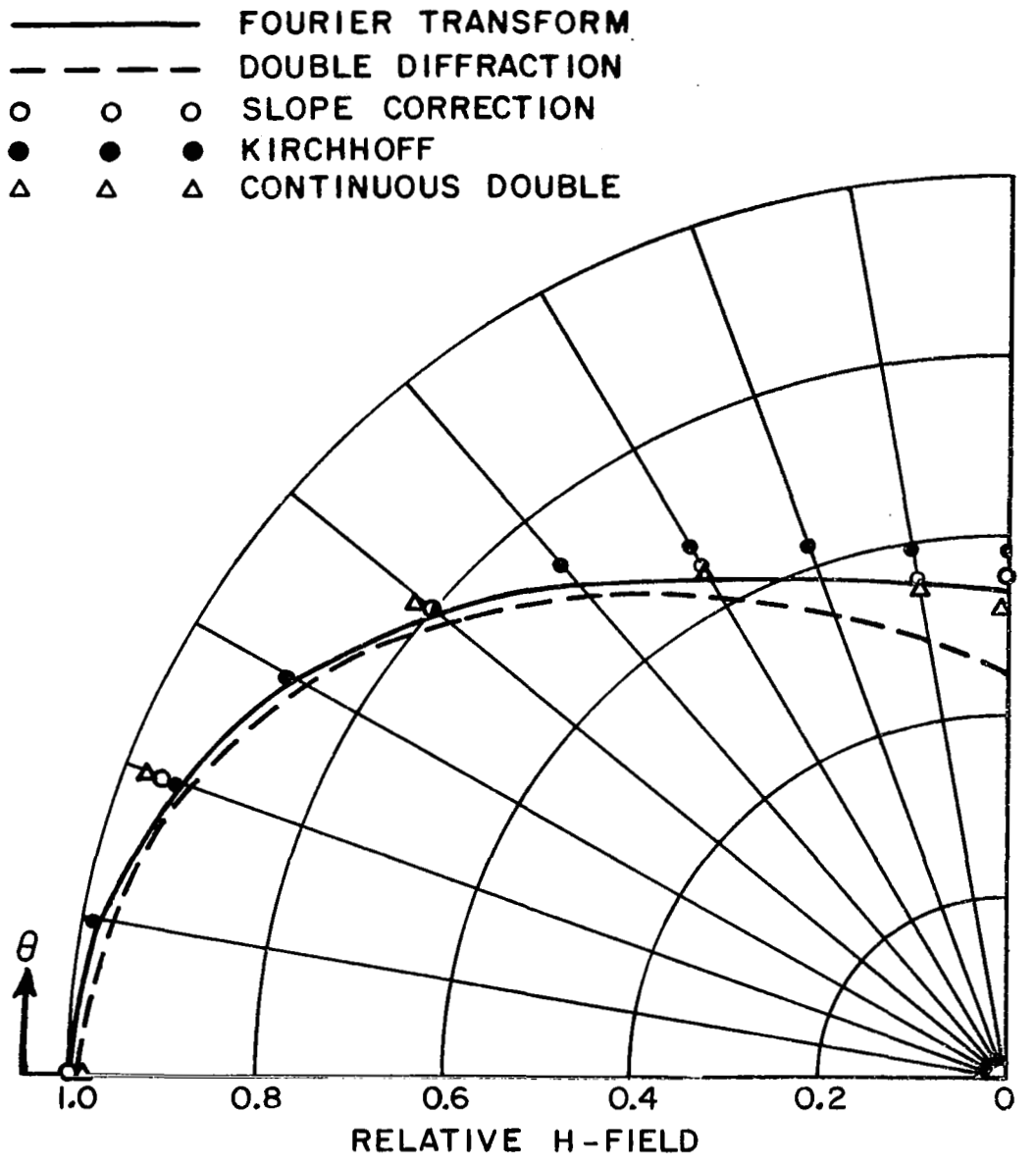

Fig. 19 - Radiation Pattern for TEM Guide (n = 1.5, $h/\lambda = 0.5411$)

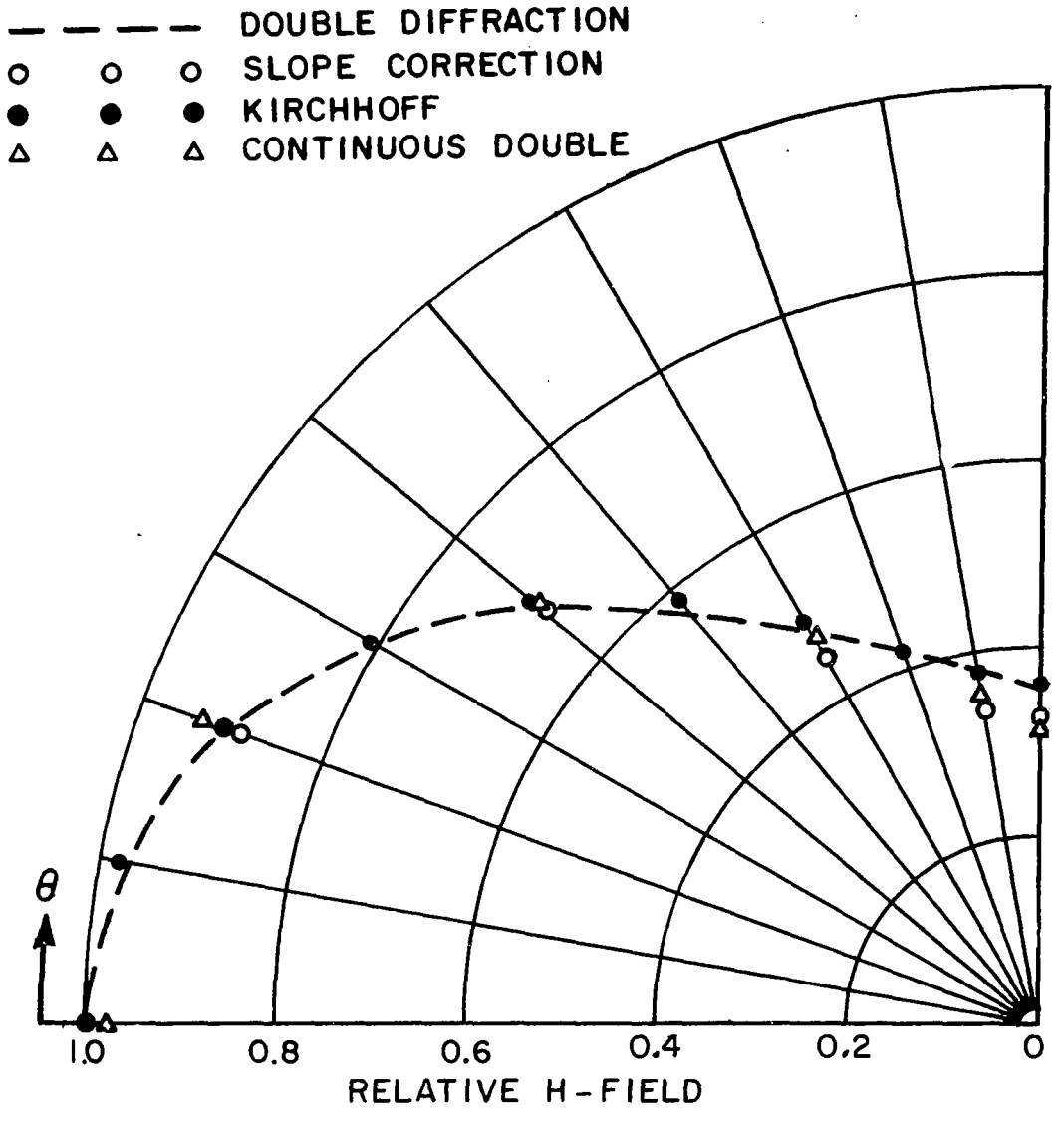

Fig. 20 - Radiation Pattern for TEM Guide (n = 1.5, $h/\lambda = 0.7$)

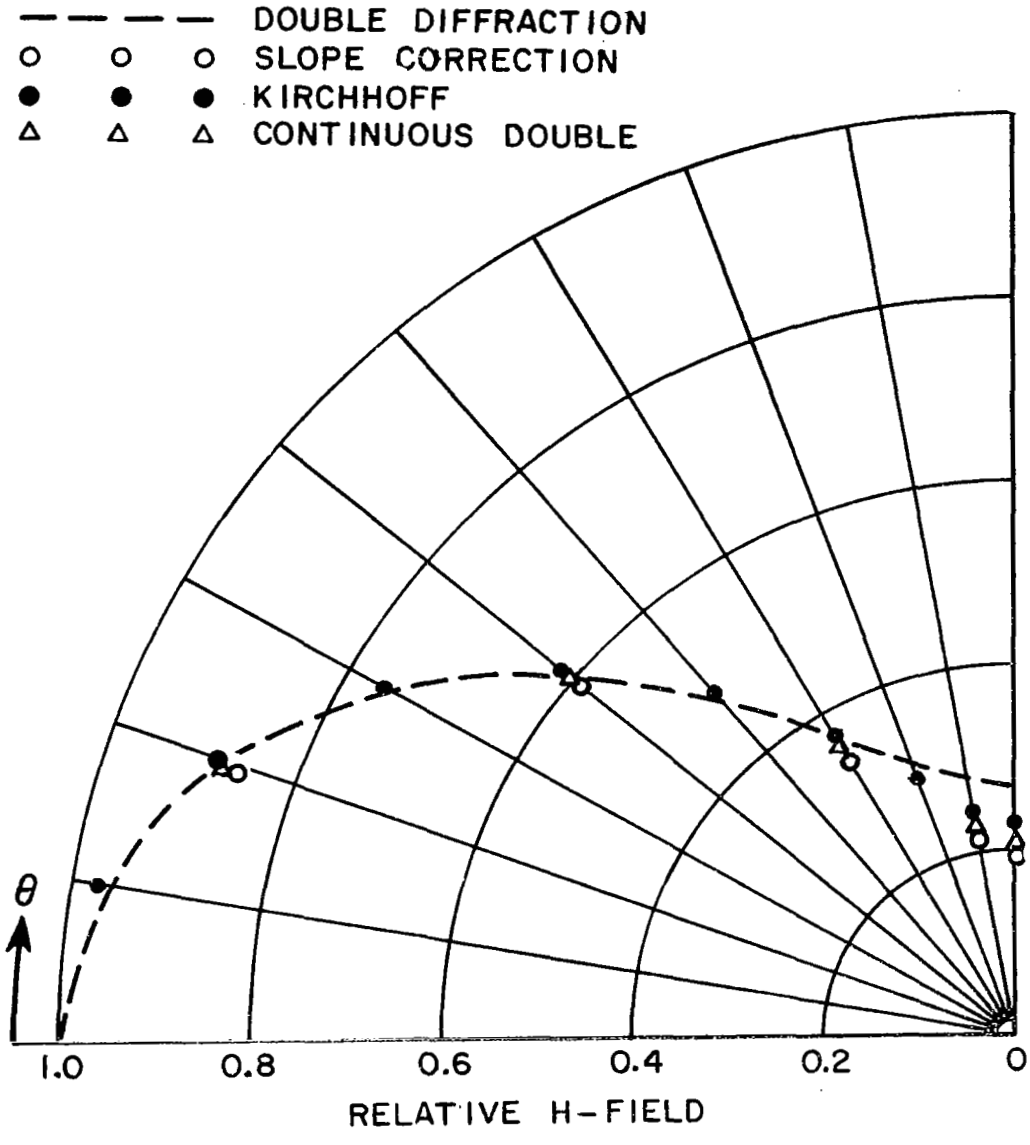

Fig. 21 - Radiation Pattern for TEM Guide ($n = 1.5$, $h/\lambda = 0.8$)

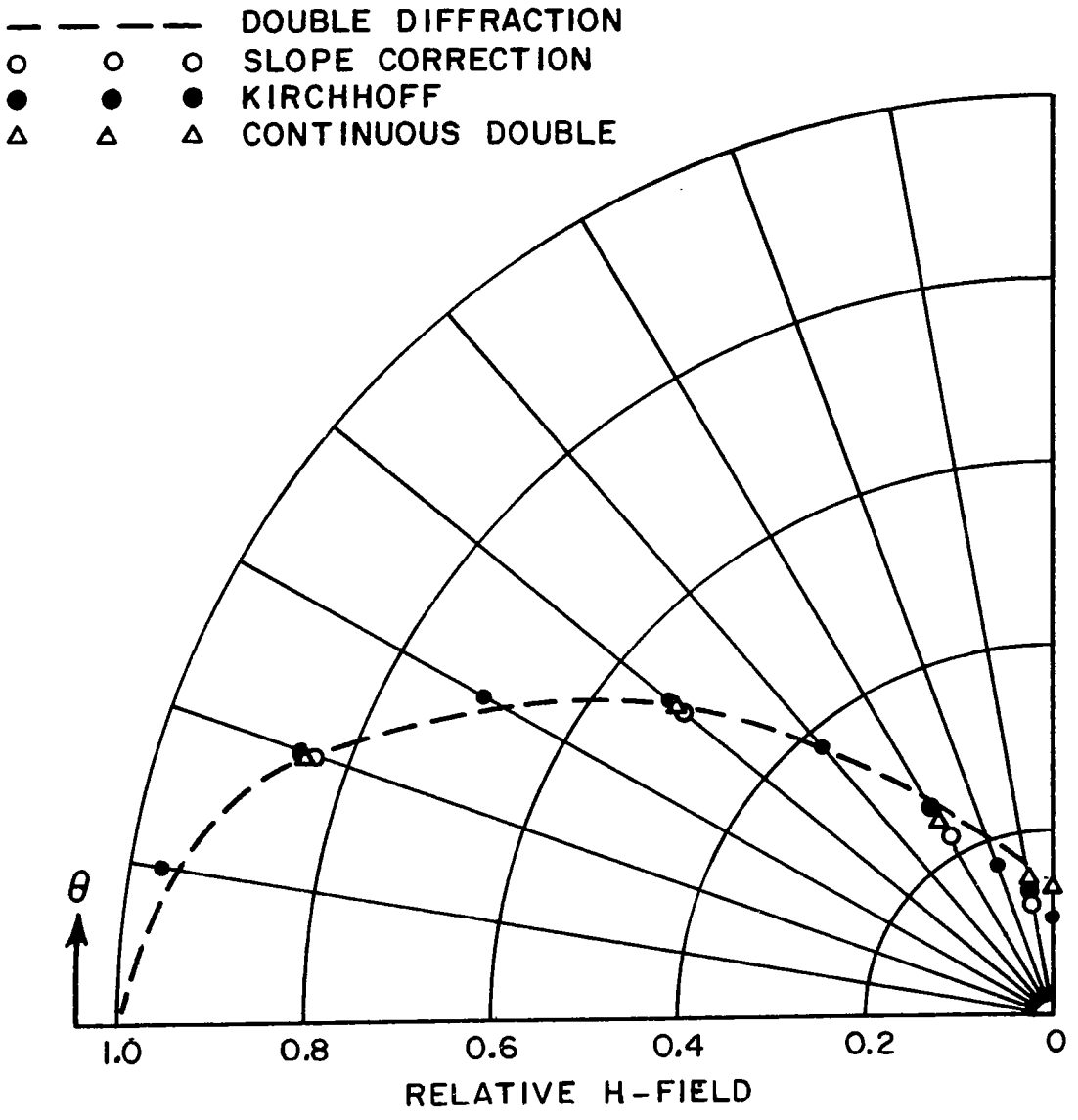

Fig. 22 - Radiation Pattern for TEM Guide ($n = 1.5$, $h/\lambda = 0.9$)

The radiation patterns are also calculated by using the Kirchhoff approximation in which the total field in the plane of the aperture is assumed to be the incident field and is zero on the remaining surface of the aperture giving

$$R(\theta) = \frac{\sin\left(\frac{1}{2} kh \sin\theta\right)}{\frac{1}{2} kh \sin\theta} \quad . \tag{29}$$

The Kirchhoff approximation is equivalent to the radiation pattern of dominant TEM mode, i.e., neglecting the higher order modes.

It is noted that the radiation patterns calculated using the slope correction term agree well with the Fourier transform analysis in the region $60° < \theta < 90°$. However, the patterns obtained by the double diffraction formulation and the continuous-double formulation do not always agree well with the Fourier transform analysis in that region. The radiation pattern of the ground-plane guide is well approximated by the double diffraction result in the region $0° < \theta < 40°$ as seen by comparison with the Fourier transform analysis and the Kirchhoff approximation. Since the higher order modes do not perturb the radiation pattern significantly in the region $0° < \theta < 40°$, the Kirchhoff approximation predicts the field well in that region. However, the higher order modes do influence the radiation pattern in the region near $\theta = 90°$. The radiation pattern calculated by the slope correction and the continuous-double formulation agree well for large values of guide width, i.e., $h = 0.7$, 0.8, and $0.9\ \lambda$, as shown in Figs. 20 to 22. Thus for large values of guide width, the continuous-double formulation yields accurate patterns.

Third and higher order diffracted waves are not included in these calculations. As seen by the accuracy of the slope diffraction analysis which only includes up to second order diffractions, the higher order diffraction effects are quite small. Furthermore, these effects are difficult to accurately analyze.

C. Parallel-Plate Guide With Wedge Angles 80°, 60°, and 20°

It has been shown that the radiation patterns of the thin-walled guide (i.e., zero wedge angle) and the ground-plane guide (i.e., 90° wedge angle) as formulated by the slope diffraction analysis agree closely with the Wiener-Hopf and the Fourier transform solutions, respectively. Since the slope correction formulation is valid for arbitrary wedge angles, the radiation patterns of symmetrical guides are plotted in Figs. 23 to 25 for a guide width $h = 0.3\ \lambda$ and for wedge angles of 80°, 60°, and 20°, respectively. Double diffraction and continuous-double results are also plotted for comparison. Similar

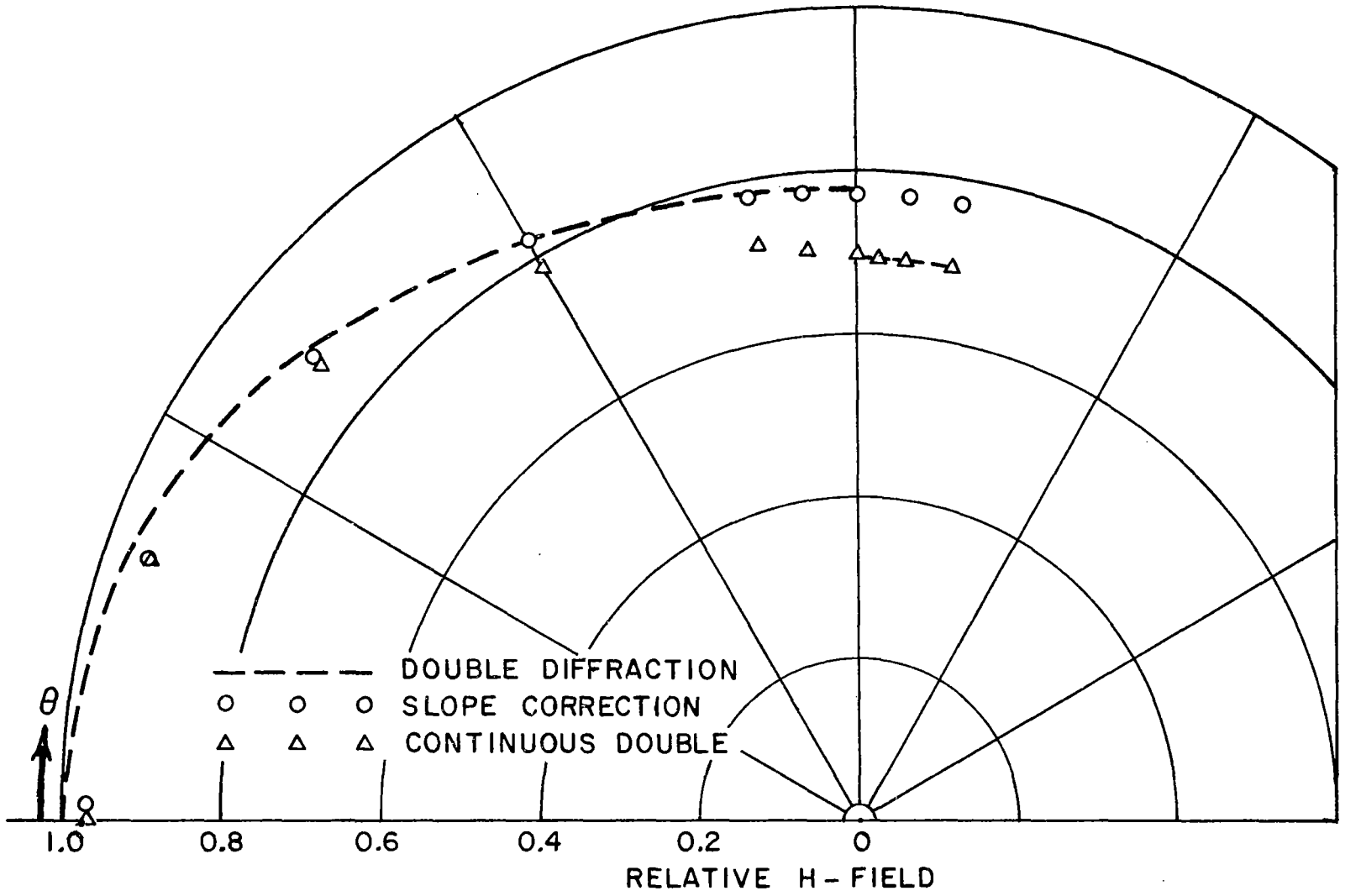

Fig. 23 - Radiation Pattern for TEM Guide ($n = \frac{14}{9}$, $h/\lambda = 0.3$)

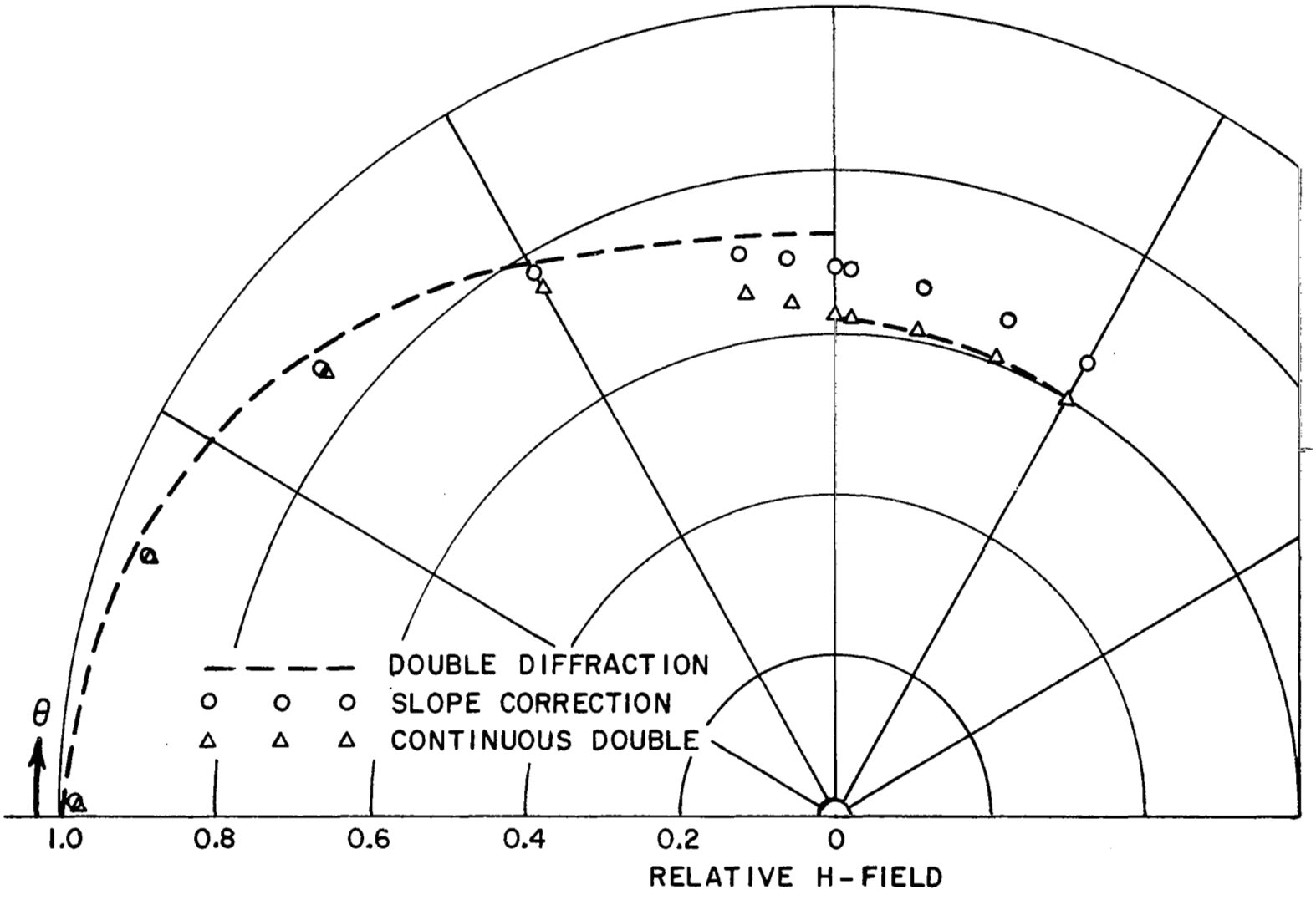

Fig. 24 - Radiation Pattern for TEM Guide ($n = \frac{5}{3}$, $h/\lambda = 0.3$)

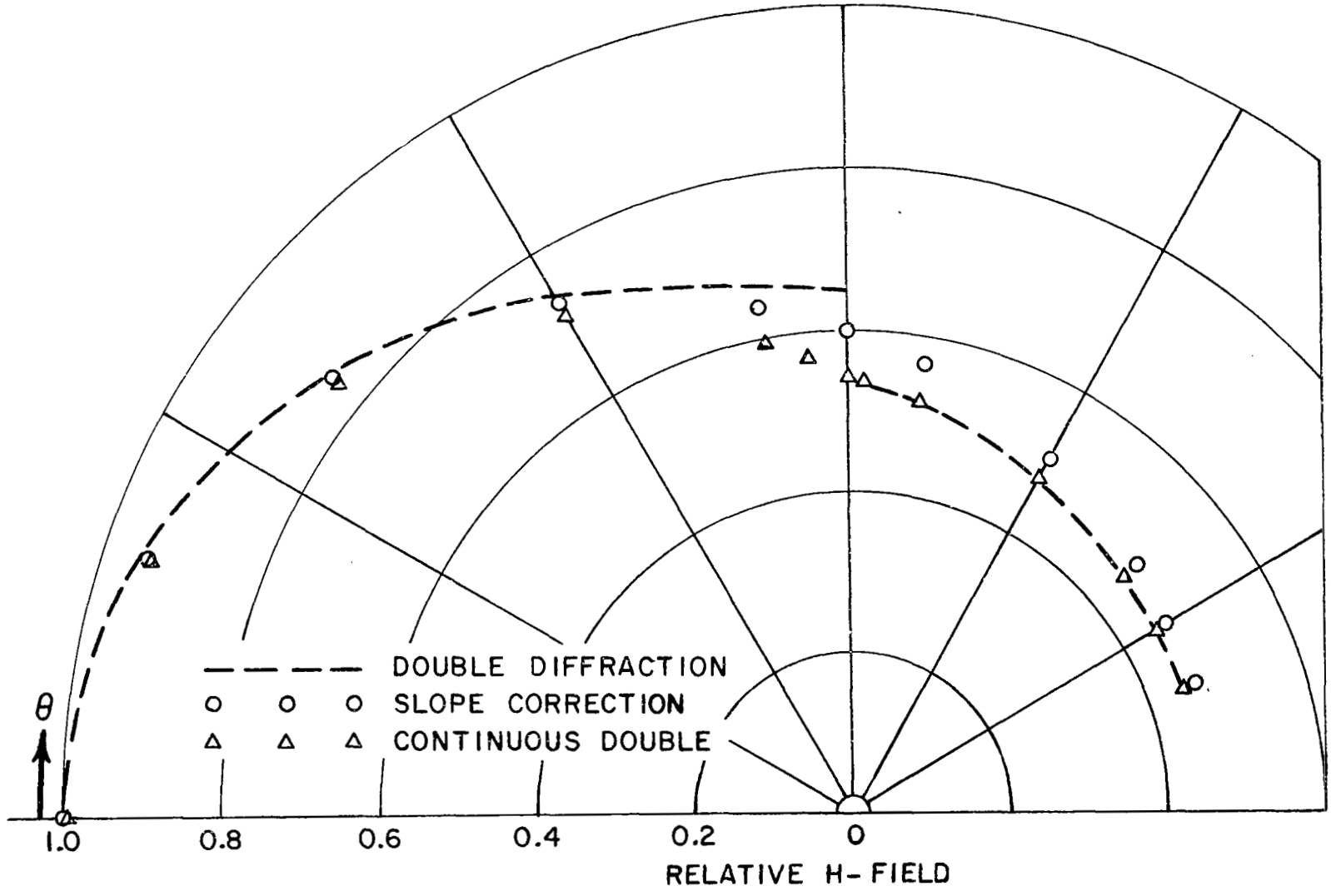

Fig. 25 - Radiation Pattern for TEM Guide ($n = \frac{17}{9}$, $h/\lambda = 0.3$)

results are plotted in Figs. 26 to 28 for a guide width $h = 0.4\ \lambda$. There are no available calculations by other methods for these wedge angles. However, based on the cases for wedge angles of 0° and 90°, it is believed that the slope diffraction formulation yields accurate results in the region near the plane of the aperture. Outside this region the radiation pattern should be well approximated by the double diffraction formulation.

V. CONCLUSIONS

In this publication the radiation pattern of the symmetrical parallel-plate TEM waveguide is calculated by a slope wave diffraction analysis. This analysis gives an improvement in the accuracy of the pattern in the region near the plane of the guide aperture, as compared to the previous wedge diffraction analysis. The comparison is based on the exact solution (Wiener-Hopf technique) for the thin-walled guide and a good approximate solution (higher order mode Fourier transform formulation) for the ground plane guide. The radiation patterns obtained using the slope diffraction analysis agree well with the above formulations except for very small guide width, i.e., $h < 0.2\ \lambda$. For large values of guide width, i.e., $h > 0.7\ \lambda$, the radiation pattern calculated by the continuous-double formulation is adequate. The slope diffraction analysis may also be applied to the unsymmetrical parallel-plate guide with arbitrary truncation angles. This technique offers a general method for analyzing diffraction by nonuniform incidence waves which occur in antenna and scattering analysis such as edge illumination of reflector antennas and interactions in slot and waveguide apertures.

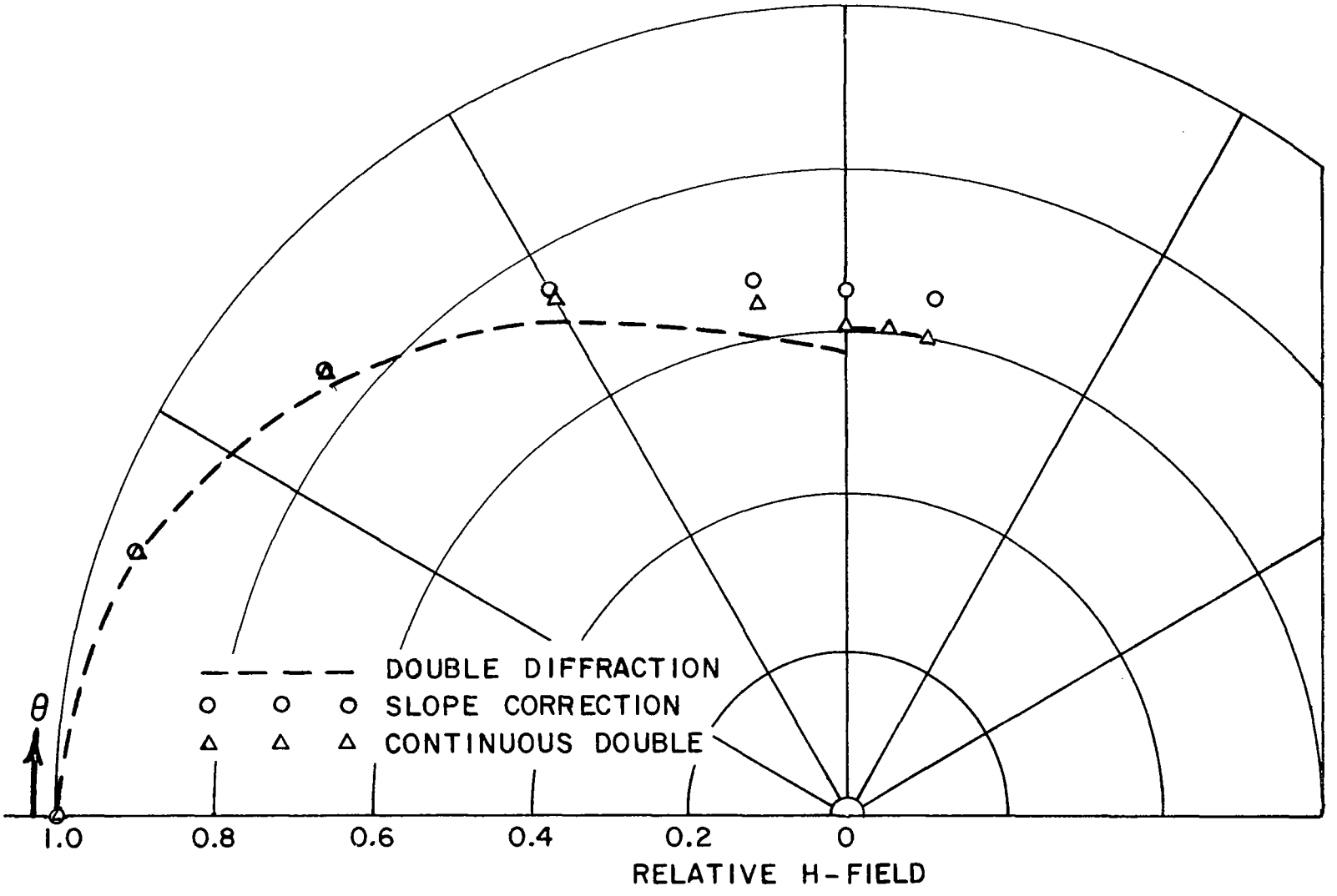

Fig. 26 - Radiation Pattern for TEM Guide ($n = \frac{14}{9}$, $h/\lambda = 0.4$)

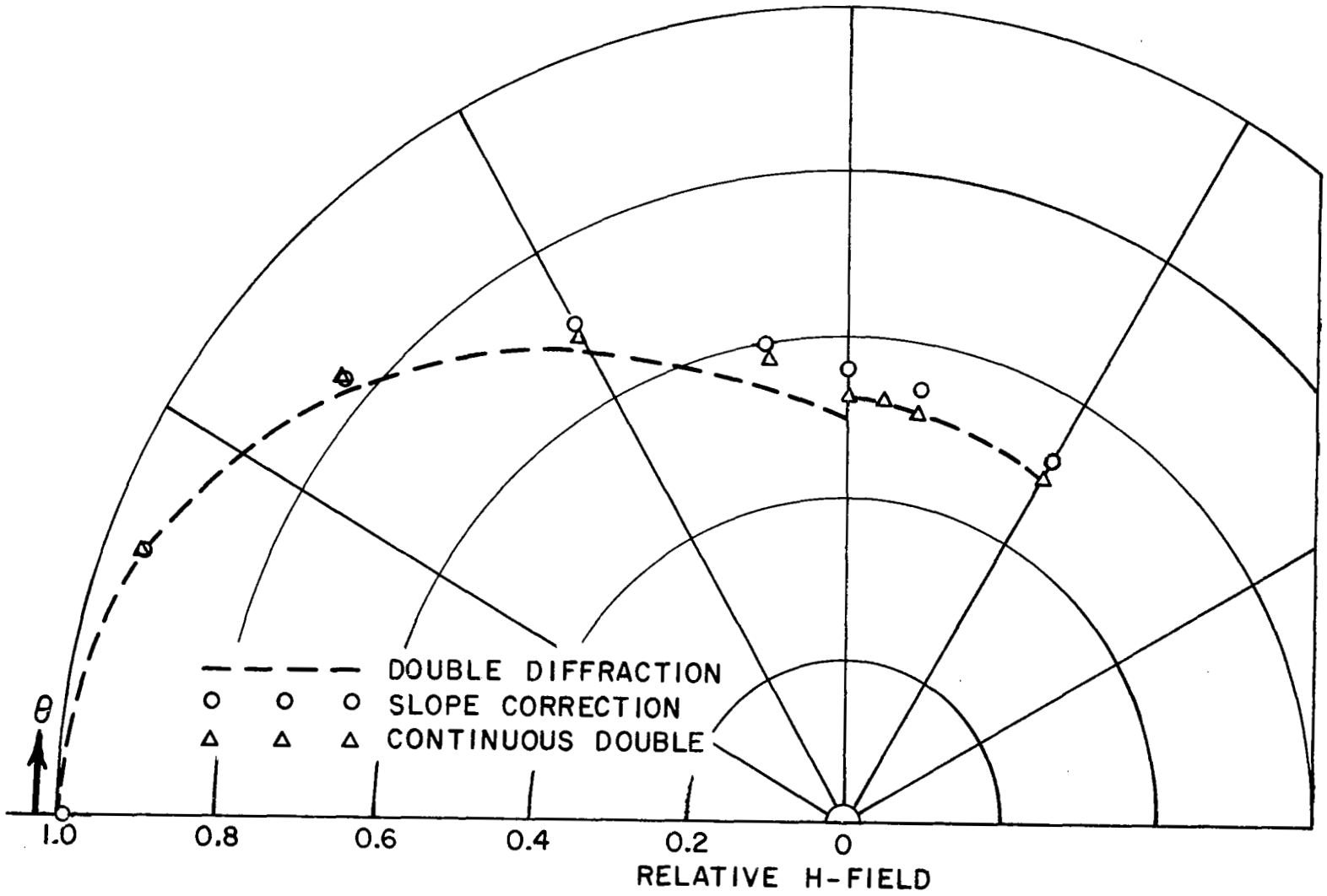

Fig. 27 - Radiation Pattern for TEM Guide ($n = \frac{5}{3}$, $h/\lambda = 0.4$)

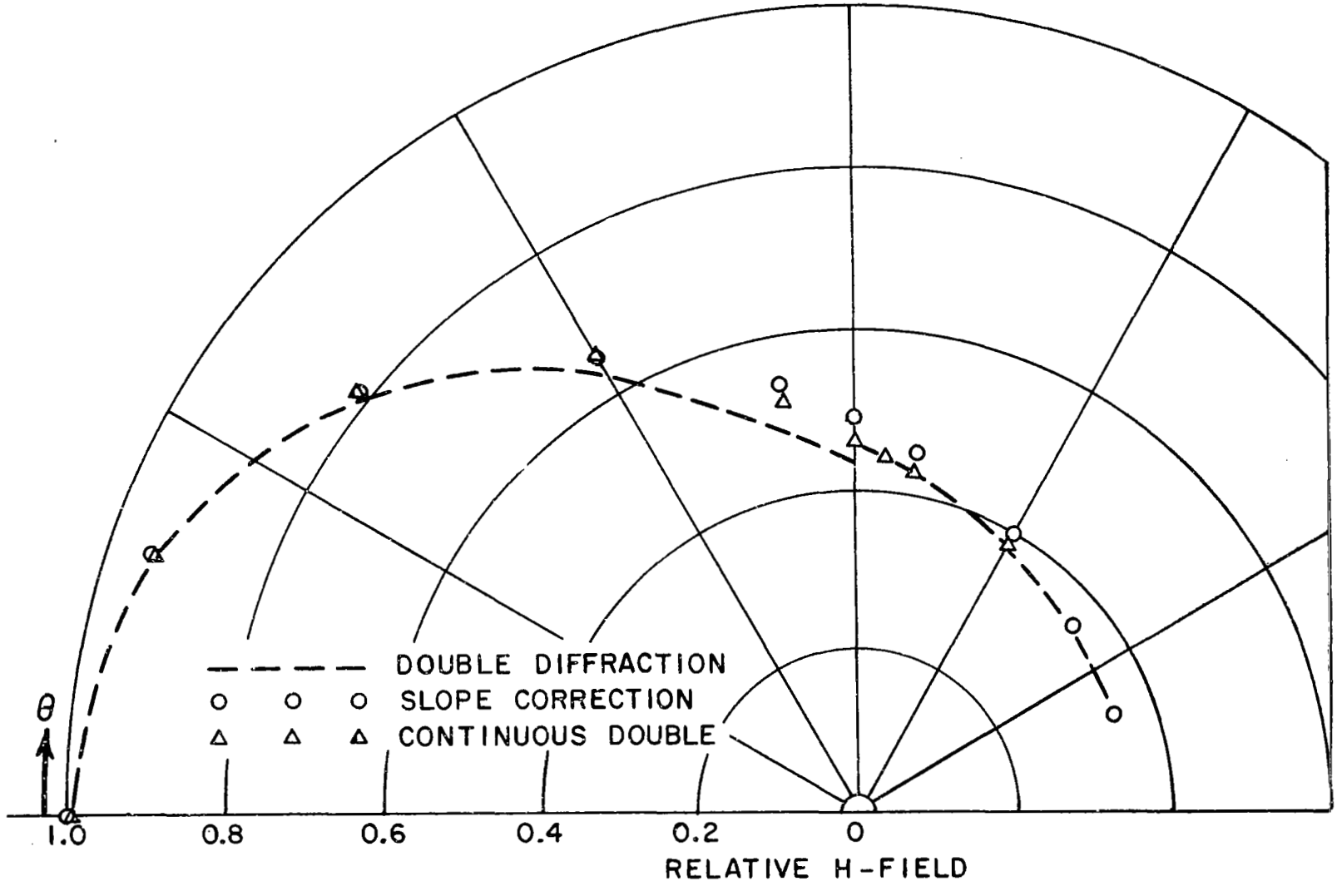

Fig. 28 - Radiation Pattern for TEM Guide ($n = \frac{17}{9}$, $h/\lambda = 0.4$)

APPENDIX

The TEM radiation pattern of a parallel-plate waveguide mounted in an infinite ground plane has been analyzed by H. M. Nussenzveig employing the Fourier transform method. Higher order modes are included in this analysis for which the wave function in the guide is given in terms of incident and reflected modes as

$$U_I(X,Y) = \cos(k_{y,s}Y)e^{-ik_{x,s}X} + \sum_{n=0}^{\infty} a_n \cos(k_{y,n}Y)e^{ik_{x,n}X} \tag{30}$$

The radiated fields of the waveguide are given by

$$U_{II}(R,\theta) \approx \tfrac{1}{2}\pi \cos\theta A(\gamma)H_0^{(2)}(kR) \quad (R \to \infty) \tag{31}$$

where the radiation pattern $A(\gamma)$ is given in terms of the modal coefficients as

$$A(\gamma) = \left(\frac{2}{\pi}\right)(1-\gamma^2)^{-\frac{1}{2}}\gamma \sin\gamma K\left[(1-a_0)\gamma^{-2} + i\sum_{n=1}^{\infty}(-1)^n(\gamma_n^2-1)^{\frac{1}{2}}(\gamma_n^2-\gamma^2)^{-1}a_n\right] \tag{32}$$

$$\text{and } \gamma = \frac{k_y}{k} = \sin\theta \tag{33}$$

$$K = \frac{\pi h}{\lambda} \tag{34}$$

$$\gamma_n = \frac{k_{y,n}}{k} = \frac{n\pi}{K} = \frac{n\lambda}{h} \tag{35}$$

The dominant mode radiation pattern reduces to the Kirchhoff approximation $R_k(\theta)$, giving

$$R_k(\theta) = \frac{\sin(\frac{1}{2}kh\sin\theta)}{\frac{1}{2}kh\sin\theta} \tag{36}$$

where the factor $\frac{\pi h\, e^{-j(kR - \frac{\pi}{4})}}{\sqrt{2\pi kR}}$ is suppressed.

The coefficients a_n as shown in Eq. (33) were calculated by C. Marcio Amaral and J. W. Bautista Vidal[11]. These coefficients are tabulated for values of guide width up to 0.6 λ.

Table IX

h	πh	a_o	a_1	a_2
0.22282	0.7	-0.1202 -j0.3418	0.04148 -j0.06963	-0.01255 +j0.02341
0.31831	1.0	-0.03218 -j0.2634	0.06704 -j0.08465	-0.01949 +j0.02889
0.35014	1.1	-0.01461 -j0.2401	0.07620 -j0.08786	-0.02191 +j0.03024
0.44563	1.4	+0.01722 -j0.1795	0.1042 -j0.09173	-0.02919 +j0.03276
0.54113	1.7	0.02905 -j0.1317	0.1305 -j0.08706	-0.03583 +j0.03309

REFERENCES

1. Rudduck, R. C., "Application of Wedge Diffraction to Antenna Theory," Report 1691-13, 30 June 1965, ElectroScience Laboratory (formerly Antenna Laboratory), The Ohio State University Research Foundation; prepared under Grant Number NsG-448, National Aeronautics and Space Administration, Office of Grant and Research Contracts, Washington, D.C.

2. Ryan, C. E., Jr., Rudduck, R. C., "Calculation of the Radiation Pattern of a General Parallel-Plate Waveguide Aperture for the TEM and TE_{01} Waveguide Modes," Report 1693-4, 10 September 1964, ElectroScience Laboratory (formerly Antenna Laboratory), The Ohio State University Research Foundation; prepared under Contract N62269-2184, U.S. Naval Air Development Center, Johnsville, Pennsylvania.

3. Yu, J. S., Rudduck, R. C., "Higher-Order Diffraction Concept Applied to Parallel-Plate Waveguide Patterns", Report 1691-16, 15 October 1965, ElectroScience Laboratory (formerly Antenna Laboratory), The Ohio State University Research Foundation; prepared under Grant Number NsG 448, National Aeronautics and Space Administration, Office of Grant and Research Contracts, Washington, D.C.

4. Noble, B., Method Based on the Wiener-Hopf Technique for the Solution of Partial Differential Equations, Pergamon Press, New York, 1958, pp. 105-110 and p. 127.

5. Wainstein, L. A. "Theory of Diffraction and Method of Factorization" (Russian), Ied. Soviet Radio, Moscow, (1966).

6. Nussenzveig, H. M., "Solution of a Diffraction Problem, I. The Wide Double Wedge, II. The Narrow Double Wedge," Philosophical Transactions of the Royal Society of London, Series A, Mathematical and Physical Sciences, No. 1003, Vol. 252, (15 October 1959), pp. 1-51.

7. Keller, J. B., "Geometrical Theory of Diffraction," J. Opt. Soc. Am., 52, No. 2 February 1962, pp. 116-130.

8. Ia. Ufimtsov, "Secondary Diffraction of Electromagnetic Waves at a Strip," J. Tech. Phys. (USSR), Vol. 28, No. 3, pp. 569-582 (1958) [CC Trans].

9. Wu, D. C., "The TEM Radiation Pattern of a Thin-Walled Parallel-Plate Waveguide Analyzed by a Surface Integration Technique," Report 1691-23, 20 September 1967, ElectroScience Laboratory (formerly Antenna Laboratory), The Ohio State University Research Foundation; prepared under Grant Number NsG-448, National